

**DEPARTAMENT DE BIOLOGIA CEL·LULAR I ANATOMIA PATOLÒGICA
FACULTAT DE MEDICINA
UNIVERSITAT DE BARCELONA**

**PROGRAMA DE DOCTORAT
BIOLOGIA I PATOLOGIA CEL·LULARS
Bienni 2002-2004**



**ANÀLISI DELS MECANISMES MOLECULARS IMPLICATS EN
EL DESENVOLUPAMENT I PROGRESSIÓ
DELS LIMFOMES DE CÈL·LULA B PETITA**

**Tesi presentada per Verònica Fernández Pascual
per optar al grau de Doctora en Biologia**

**Director de tesi: Dr. Elías Campo Güerri
Tutor: Dr. Carles Enrich Bastús
Barcelona 2008**

El món exigeix resultats.

No expliquis als altres els teus dolors de part. Ensenya'ls el nen. (*Indira Gandhi*)

Si busques resultats diferents, no facis sempre el mateix (*Albert Einstein*)

RESULTATS

TREBALL 1: PROLIFERACIÓ EN NHL

Un model de cinc gens pot predir la supervivència del limfoma de cèl·lules del mantell i aplicar-se en teixit fixat amb formol i inclòs en parafina

Journal of Clinical Oncology, 2007 (en revisió)

(Journal impact factor 2006: 13.598)

L'augment de l'expressió de MDM2 s'associa amb menor supervivència en el limfoma de cèl·lules del mantell, però no es relaciona amb la presència del SNP309

Haematologica 2007, 92: 574-575

(Journal impact factor 2006: 5.032)

Un model de cinc gens pot predir la supervivència del limfoma de cèl·lules del mantell i aplicar-se en teixit fixat amb formol i inclòs en parafina

Objectius. Tot i la presència de la translocació t(11;14) que afecta el gen de la CCND1 i que es troba en pràcticament tots els casos de limfoma de cèl·lules del mantell (MCL), el curs clínic de la malaltia és molt variable. L'objectiu del present estudi és desenvolupar un model quantitatiu basat en l'expressió gènica per predir la supervivència de pacients amb MCL acabats de diagnosticar, format pel mínim nombre de gens i que es pugui aplicar en mostres tumorals fixades en formol i incloses en parafina (FFPE, de l'anglès *Formalin-Fixed and Paraffin-Embedded*). **Material i Mètodes.** L'expressió de 33 gens amb potencial impacte pronòstic i patogènic es va analitzar mitjançant la reacció en cadena de la polimerasa quantitativa a temps real (qPCR) en un format d'array de baixa densitat (targetes microfluídiques) en mostres tumorals congelades de 73 pacients amb MCL. Es van aplicar mètodes Cox multivariants i algorismes *stepwise* per construir predictors de supervivència basats en l'expressió gènica, obtenint un model optimitzat de cinc gens. Aquest predictor es va aplicar posteriorment en mostres tumorals en FFPE de 13 pacients amb MCL de la sèrie inicial i en 42 mostres de MCL d'una sèrie independent. **Resultats.** El predictor de supervivència optimitzat es componia dels 5 gens RAN, MYC, TNFRSF10B, POLE2 i SLC29A2, i es va validar per l'aplicació en mostres de teixit en FFPE. Va permetre la predicció de la supervivència de pacients amb MCL amb diferent pronòstic clínic i va demostrar ser més acurat que el marcador immunohistoquímic Ki67, molt usat en MCL. **Conclusions.** Presentem un test basat en qPCR que permet la predicció de la supervivència dels pacients de MCL i que es pot aplicar tant en material congelat com en FFPE. Aquest predictor pot esdevenir molt útil pel desenvolupament d'aproximacions terapèutiques individualitzades pels pacients de MCL.

* La contribució personal en aquest treball ha estat la participació en el disseny experimental del projecte, l'extracció de material genètic de les mostres (RNA) i posterior anàlisi de l'expressió gènica de certs gens mitjançant la tecnologia de la PCR quantitativa a temps real (qPCR); així com la interpretació dels resultats i la redacció del treball.

A FIVE-GENE MODEL TO PREDICT SURVIVAL IN MANTLE CELL LYMPHOMA AND ITS APPLICATION TO FORMALIN-FIXED PARAFFIN-EMBEDDED TISSUE

Elena Hartmann^{1*}, Verònica Fernández^{2*}, Victor Moreno³, Joan Valls³, Luis Hernández², Francesc Bosch⁴, Pau Abrisqueta⁴, Wolfram Klapper⁵, Martin Dreyling⁶, Eva Hoster⁶, Hans Konrad Müller-Hermelink¹, German Ott¹, Andreas Rosenwald^{1#}, Elías Campo^{2#}

¹Institute of Pathology, University of Würzburg, Germany

²Hematopathology Section, Department of Pathology, Hospital Clinic, Institut d'Investigacions Biomediques August Pi i Sunyer, University of Barcelona, Barcelona, Spain

³Unit of Biostatistics and Bioinformatics, Cancer Epidemiology Service, Institut Català d'Oncologia-Institut d'Investigació de Bellvitge (IDIBELL)

⁴Department of Hematology, Hospital Clinic, University of Barcelona, Barcelona, Spain

⁵Institute of Pathology, University of Kiel, Germany

⁶Department of Internal Medicine III, University of Munich, Germany

***E.H. and V.F. contributed equally to this work.**

#E.C. and A.R. are co-senior authors of this study.

Short running title: gene expression-based predictor of survival in MCL

Keywords: mantle cell lymphoma, survival, multiple gene predictor, low-density array, FFPE

Word count: 2994

Corresponding author: Andreas Rosenwald, M.D.; Institute of Pathology, University of Würzburg; Josef-Schneider-Str. 2; 97080 Würzburg, Germany

Grant support: V.F. is a recipient of a predoctoral fellowship from the Spanish Ministry of Education and Science (MEC). A.R. and E.H. are supported by the Interdisciplinary Center for Clinical Research (IZKF), University of Wuerzburg, Germany. L.H. is supported by FIS 01/3046. The study was also supported by the European Grant No. 503351 (European Mantle Cell Lymphoma Network, A.R., E.C., G.O.), the Lymphoma Research Foundation (LRF), USA (A.R., E.C.) and the grant CICYT SAF 05/5855 by

the Spanish Ministry of Science (E.C.) and ISCIII-RETIC RD06/0020 by the Spanish Ministry of Health (EC, VM).

Author contribution: E. Hartmann and V. Fernández extracted RNA from the frozen and FFPE tumor samples and performed the expression analysis of the given genes by real time quantitative PCR. V. Moreno and J. Valls did the statistical analysis. L. Hernandez participated in the selection of the genes and the design of the low-density array platform. E. Campo, G. Ott, H.K. Müller-Hermelink, F. Bosch, P. Abrisqueta and A. Rosenwald selected and reviewed the MCL samples; W. Klapper and M. Dreyling provided additional samples for the FFPE validation set on behalf of the German Low-Grade Lymphoma Study Group. E. Campo and A. Rosenwald designed and supervised the whole project. E. Hartmann and V. Fernández drafted the manuscript and A. Rosenwald and E. Campo wrote the final version. All authors reviewed critically the final version of the manuscript.

Conflict of interest notification: The authors state that no potential conflicts of interest exist in the present manuscript.

ABSTRACT

Purpose: Despite the common underlying translocation t(11;14) involving *Cyclin D1* that is present in nearly all cases of mantle cell lymphoma (MCL), the clinical course of the disease is highly variable. The aim of the present study was to develop a quantitative gene expression-based model to predict survival in newly diagnosed MCL patients involving a minimum number of genes and applicable to formalin-fixed paraffin-embedded (FFPE) tumor samples.

Patients and Methods: The expression of 33 genes with potential prognostic and pathogenetic impact in MCL was analysed using quantitative reverse-transcription polymerase chain reactions (qRT-PCR) in a low density array format in frozen tumor samples from 73 MCL patients. Multivariate Cox methods and stepwise algorithms were applied to build gene expression-based survival predictors. An optimized 5-gene-model was subsequently applied to FFPE tumor samples from 13 MCL patients from the initial series and to 42 independent MCL samples.

Results: The optimized survival predictor was composed of the 5 genes *RAN*, *MYC*, *TNFRSF10B*, *POLE2* and *SLC29A2* and validated for application in FFPE tissue samples. It allowed the survival prediction of MCL patients with widely disparate clinical outcome and was superior to the immunohistochemical marker Ki-67, an established prognostic factor in MCL.

Conclusion: We here present a validated qRT-PCR based test for survival prediction in MCL patients that is applicable to fresh frozen as well as to FFPE tissue specimens. This test may prove useful to guide individualized treatment approaches for MCL patients.

INTRODUCTION

Mantle cell lymphoma (MCL) is a distinctive subtype of B-cell non-Hodgkin's lymphoma (B-NHL) characterized by the translocation $t(11;14)(q13;32)$ and the overexpression of Cyclin D1¹⁻³. The clinical course of these patients can be highly variable. In general, MCL shows an aggressive clinical behaviour with poor response to current therapeutic approaches^{2,4}, and the median survival of MCL patients following diagnosis is between 3 and 5 years. However, some patients succumb to their disease in less than 6 months, while others survive more than 10 years. The current treatment approaches for MCL patients are rather uniform and rarely reflect the widely varying clinical behavior. However, before more individualized and risk-adapted treatment strategies can be tested in prospective clinical trials, it is a prerequisite to develop molecular tests for newly diagnosed MCL patients that reliably predict their clinical course and that are applicable in a routine diagnostic setting.

In the recent years, many attempts have been made to identify clinical, histological and molecular markers that allow the stratification of MCL patients into different risk groups. Morphologically, two major variants of MCL have been identified, namely the typical or classical and the blastoid variants, and blastoid MCL cases show a worse clinical outcome^{5,6}. Genetically, alterations affecting the cell cycle machinery and the DNA damage response pathways appear to be the hallmarks of MCL¹⁻³. Secondary genetic alterations in MCL frequently target key regulators of these pathways and are also associated with inferior clinical outcome⁷⁻¹².

The strongest predictor of survival in MCL patients was identified by gene expression profiling in a large series of MCL¹³. In particular, a gene expression-based molecular predictor consisting of 20 proliferation-associated genes was constructed that allowed the definition of prognostic subgroups of MCL patients in which the median survival differed by almost 6 years. This survival predictor was shown to be superior to other prognostic molecular markers either alone or in combination and was therefore viewed as an integrator of multiple oncogenic events¹³. It is obvious that a microarray-based technical platform is currently not feasible for routine clinical application and, accordingly, the potential surrogate marker Ki-67 measured by immunohistochemistry has attracted major attention recently. In several studies, increased Ki-67 indices in MCL tumor cells were related to a shorter survival of the patients¹⁴⁻¹⁶ and measurement of the tumor cell proliferation by Ki-67 is now part of the routine diagnostic procedure in many lymphoma centers. However, immunohistochemical techniques are only semiquantitative in nature and, in a recent multi-center immunohistochemistry study,

the concordance of the staining and scoring procedures for Ki-67 between several experienced laboratories was less than satisfactory¹⁷.

The aim of the present study was therefore to develop an accurate and quantitative gene-expression based survival model for MCL patients that involves a minimum number of genes and is applicable in a routine diagnostic setting to formalin-fixed paraffin-embedded (FFPE) tissue specimens from MCL patients.

MATERIAL AND METHODS

Case selection

Frozen tumor samples from 73 newly diagnosed mantle cell lymphoma (MCL) patients were obtained from the Institute of Pathology, University of Würzburg and the Hospital Clínic, University of Barcelona. 15 of the 73 MCL specimens had been included in a previous, gene expression-based study¹³. Corresponding formalin-fixed and paraffin-embedded (FFPE) tumor samples from 13 of the 73 MCL patients as well as FFPE tissue samples from 57 independent MCL cases, including 22 cases from the Institute of Pathology in Kiel, were also obtained for further validation purposes. Of these, 42 tumors had amplifiable cDNA. The diagnosis was established according to the WHO criteria¹⁸, and the study was approved by the local Institutional Review Boards (IRB). Among the 73 MCL cases with available frozen material, 54 showed typical morphology and 19 corresponded to the blastoid variant. Within the independent set of 42 FFPE MCL cases, 35 were typical and 7 were blastoid variants. Immunohistochemical staining for Ki-67 and evaluation of the proliferation fraction was performed as previously described¹⁵ (Table 1, Supplementary Table 1).

RNA extraction and reverse-transcription PCR

RNA from frozen samples was extracted using the TRIzol[®] reagent following the manufacturer's instructions (Invitrogen Life Technologies[®], Carlsbad, CA, USA). RNA from FFPE samples was extracted as previously described with minor modifications¹⁹. A detailed protocol is provided in the supplementary information. RNA integrity was examined with the Agilent 2100 Bioanalyser (Agilent Technologies[®], Palo Alto, CA, USA). Complementary DNA synthesis was carried out from 1 µg of total RNA with the High Capacity cDNA Archive Kit (Applied Biosystems[®], Foster City, CA, USA) as recommended by the supplier.

Real time quantitative RT-PCR (qRT-PCR)

The expression of 33 genes with potential prognostic and pathogenetic impact in MCL was analyzed using a custom TaqMan[®] low-density array platform (Micro Fluidic Cards, Applied Biosystems[®]). In particular, the selection included genes implied in the proliferation signature¹³, cell cycle^{2,20-24}, apoptosis²⁵⁻³¹, nucleoside transport³² and metabolism processes^{33,34}. The chosen pre-developed assays are summarized in Table 2. QRT-PCR was performed using the ABI Prism[®]7900 HT Sequence Detection System under standard conditions (Applied Biosystems[®]). The raw data analysis was carried out with the Sequence Detector System (SDS) software version 2.1 (Applied Biosystems[®]). Two control genes were included in the study: 18S (mandatory for the technique) and β 2-microglobulin (B2M, chosen according to previous work¹³). Gene expression levels were further calculated with the $2^{-\Delta\Delta Ct}$ method by using 18S and B2M as endogenous controls³⁵ (Supplementary Table 2). One MCL case of the series was used as mathematical calibrator. For optimal qRT-PCR performance in FFPE material the amplicon sizes were reduced to less than 80bp in the four genes that was required. Therefore, optimized pre-developed assays were chosen for SLC29A2 (Hs01546959_g1) and TNFRSF10B (Hs01043164_m1), and probe/primer sets were modified (using the Primer Express[®] software, Applied Biosystems[®]) for MYC (Probe: 5'-CTTAGAGGTTGCTCAGACAA-3', Primer forward: 5'-GGCAGCACAGTATGAGCACG-3', Primer reverse: 5'-ATCCTCATCCGGGAGAGCA-3') and RAN (Probe: 5'-AGGAGGAACAAGAAGAT-3', Primer forward: 5'-CACCACCAGCAGCGACTCT-3', Primer reverse: 5'-ACAGAAACAACATCGATTTCTTCCT-3'). Gene expression levels were calculated as described above using *B2M* as a housekeeping gene. The amplicon for *POLE2* was already less than 80 bp (Table 2)

Statistical analysis

Survival was estimated with Kaplan-Meier method and compared by log rank tests. Multivariate Cox's proportional hazards models were used to identify the best subset of genes with prognostic value. Hazard ratios and 95% confidence intervals were estimated from the models and likelihood ratio tests were used to assess statistical significance. The predictive accuracy was calculated using the area under the ROC (Receiver Operating Characteristic) curve (C-index) derived from the Sommers' D statistic adapted for censored observations. Bootstrap internal validation of the stepwise selection procedure was used to assess the predictive accuracy corrected for overfitting. P-values less than 0.05 were considered significant.

RESULTS

Characteristics of MCL patients

The clinical and histological details, survival data and information on the Ki-67 index for each patient are provided in Table 1 and in the Supplementary Table 1. Importantly, no differences were observed between the frozen and FFPE MCL specimens regarding the distribution of median age, sex, histological features, median survival and median Ki-67 index (Table 1). The vast majority (78%) of MCL patients received an anthracyclin-based (CHOP-like) therapy as first-line treatment, 10% received an intensified chemotherapy regimen (mostly hyperCVAD), 6% did not receive chemotherapy and in 6% the therapy was unknown. No differences in gender distribution, histological features and overall survival were observed between the treatment groups. The group with intensified treatment included more younger patients ($p=0.002$) and was enriched for tumors with increased proliferation rates ($Ki-67 \geq 40\%$), although this feature was not statistically significant ($p=0.07$).

Development of a quantitative real time RT-PCR based predictor of survival in frozen MCL specimens

A flow-chart demonstrating the set-up of the entire study is provided in Figure 1. First, we investigated the gene expression levels of the selected 33 genes (Table 2) in fresh frozen tumor samples from 73 MCL patients by qRT-PCR in order to build a quantitative predictor of survival in frozen specimens. In a univariate analysis using B2M as a control gene, 10 out of 33 genes showed significant association with survival, and these genes are marked with an asterisk in Table 2 ($p\text{-value} < 0.05$). When using 18S as a control gene, the gene expressions of these 10 genes were also significantly associated with survival demonstrating the robustness of the chosen reference genes and the array platform. Two additional genes showed borderline significance (CDC2, $p=0.053$ and TUBA1B, $p=0.054$). Importantly, all of these genes are involved in the biological process of proliferation and 10 of the 12 genes were included in the gene expression-based proliferation signature described earlier¹³. This finding highlights the prognostic value of the proliferation signature in MCL tumor specimens and confirms its value in a large independent series of cases.

When stepwise statistical methods were applied to the data set using bootstrap replication samples, the most frequently selected genes in prognostic models comprising between one and five genes were the following: MYC (45%), RAN (35%), SLC29A2 (31%), HPRT1 (28%), POLE2 (26%), TNFRSF10B (25%) and CDKN3 (24%). Using the gene expression data from these genes, all possible models were

fitted and those with the smaller prediction error were kept. The best survival predictor was composed of the five genes RAN, MYC, TNFRSF10B, POLE2 and SLC29A2 (C-index=0.762, C-index corrected for overfitting using bootstrap= 0.71, 95%CI= 0.65-0.76) (Table 3, Figure 2 and Supplementary Table 2). Whereas RAN, MYC and TNFRSF10B were essential for the predictor, POLE2 and SLC29A2 could be replaced by other genes with similar predictive capacity (data not shown). Interestingly, the addition of up to two more genes did not improve the predictive accuracy of the five-gene model (Figure 2). In the model, increased expression levels of RAN, MYC, POLE2 and SLC29A2 were correlated with inferior survival, whereas higher levels of TNFRSF10B were associated with improved survival. Since all five genes included in the model had similar coefficients, a simplified prognostic score was calculated using identical coefficients (+1; -1 for TNFRSF10B). The application of this model resulted in the definition of MCL subgroups that differed in median survival for more than 5 years (Figure 3A, logrank p-value=1.1e⁻⁰⁶). Since tumors with elevated Ki-67 indices were enriched (but not statistically different) among MCL patients with intensified treatment, adjustment of the model for treatment resulted in a p-value of similar significance (logrank p-value=1.7e⁻⁰⁷). The five-gene predictor and the Ki-67 index were shown to be correlated (Pearson correlation=0.58). However, both provided significant independent prognostic value in a multivariate model with both factors. Importantly, the five-gene predictor was superior compared to the predictive power of the Ki-67 proliferation index (p-value <0.0001 for the five-gene predictor adjusted for Ki-67). Vice versa, the Ki-67 index also added independent prognostic information to the five-gene predictor, but to a much lesser extent (p-value=0.01 for Ki-67 adjusted for the five-gene predictor).

Application of the five-gene-predictor to routinely formalin-fixed paraffin-embedded (FFPE) tissue

To evaluate the potential of the five-gene model for widespread application in a routine diagnostic setting, we tested the qRT-PCR-based predictor in a series of routinely formalin-fixed paraffin-embedded (FFPE) MCL samples (Figure 1 and Supplementary Table 2). For 4 out of the 5 genes in the model, the amplicon length of the pre-developed assays chosen for the low-density array platform (Micro Fluidic Cards) was longer than 100 bp. These amplicons show very late or no amplification in FFPE samples. For this reason, the assays were slightly modified to shorten the amplicon size and to optimize the yield of the qRT-PCR, as described in the Material and Methods section. In a first step, a randomly selected set of 22 frozen MCL samples, that were part of the initial series, were used to test the modified qRT-PCR assays.

This analysis demonstrated an excellent correlation between the original pre-developed and modified assays (p -value <0.0001). In a second step, 18 cases from the initial series were selected with available FFPE tumor tissue obtained from the same diagnostic biopsy and subsequently analysed using the optimized assays. 13 out of these 18 samples (72%) showed successful amplification for all five genes using the modified qRT-PCR assays. Although FFPE samples generally amplified at higher C_T values, the normalized gene expression levels obtained from RNA extracted from FFPE tissue were comparable to those obtained from frozen tissues (Pearson correlation=0.77, $p=0.002$).

Validation of the five-gene survival predictor in an independent series of FFPE

MCL tumor samples

For further validation in an independent data set, we examined the performance of the five-gene predictor in an additional series of 57 MCL specimens with clinical data and FFPE tissue blocks available. 42 out of the 57 FFPE samples (74%) were amplifiable for all five genes of the model (Table 1, Supplementary Table 1 and Supplementary Table 2). Importantly, the success rate among more recent cases (1998-2003) collected as part of prospective clinical trials was 86%. In this independent series of cases, the model successfully predicted survival of MCL patients (logrank p -value=0.011). For illustration, Kaplan-Meier curves are displayed in Figure 3B showing two subgroups that differ in median survival of more than 3 years (Figure 3B). It is noteworthy however, that the five-gene model predicts survival in a linear fashion with a definite predicted survival time for each individual patient. In the validation series, the Ki-67 proliferation index was also a significant predictor of survival (p -value=0.008).

DISCUSSION

Mantle cell lymphoma (MCL) shows a widely varying clinical behavior, but current treatment approaches are rather uniform for most patients newly diagnosed with this lymphoid neoplasm. Depending on the patient's eligibility, MCL may be treated by combined immunochemotherapy followed by stem cell transplantation or by immunochemotherapy alone³⁶. However, given that the survival of MCL patients ranges anywhere between a few months and more than ten years, risk-adapted therapeutic approaches could be tested in future clinical trials. Obviously, such strategies will require the development of precise and clinically applicable tests at the time of diagnosis that would reliably predict the clinical course of the disease. In the search for clinical, histological and molecular prognostic predictors, several features

have been identified that appear to be correlated with clinical aggressiveness¹. In particular, the blastoid variant of MCL^{5,6}, deletions affecting the INK4a/ARF locus^{21,37}, inactivation of the p53 gene⁷⁻⁹, altered expression of MDM2^{20,38,39} and point mutations and genomic deletions in the *Cyclin D1* gene locus⁴⁰ are associated with inferior survival. On the mRNA expression level, increased expression of c-myc has been described in MCL patients with poor outcome⁴¹.

The strongest predictor of survival described to date in MCL patients appears to be the proliferation signature measured by gene expression profiling¹³. Since microarray-based clinical tests require the availability of fresh frozen tumor tissue, immunostaining for Ki-67 that can be performed on routinely obtained formalin-fixed and paraffin-embedded (FFPE) specimens was viewed as a good surrogate marker for the proliferative activity of the tumor cells in recent years. Indeed, the Ki-67 index is able to define risk groups among MCL patients, as described in several studies¹⁴⁻¹⁶. However, most of the published series represent investigations conducted by single institutions, and, in a recent multi-center immunohistochemistry study, the inter-laboratory variation of the staining and scoring procedures for Ki-67 was surprisingly high¹⁷. Moreover, there is evidence that a quantitative measurement of proliferation-associated gene expression levels may be superior in their predictive capacity to immunohistochemical techniques that are at most semiquantitative¹³.

To predict the clinical course of MCL patients at the time of diagnosis, we here present a molecular test that is quantitative in nature, comprises the gene expression measurements of only five genes and is applicable in most MCL cases with available FFPE tissue. The five-gene model is composed of the genes *RAN*, *MYC*, *TNFRSF10B*, *POLE2* and *SLC29A2*; this model predicts survival more precisely than any combination of fewer genes (between 1 and 4) or the Ki-67 index, whereas the addition of up to two additional genes does not improve the predictive power any further. High expression of *RAN*, *MYC*, *POLE2* and *SLC29A2* is related to a worse prognosis, while increased expression of *TNFRSF10B* correlates with a more favorable clinical course. There is no indication that the validity of the model may be affected by the heterogeneity of treatments in our cohort, since all biological and clinical parameters (except for age) were equally distributed between the different treatment groups. In addition, the model maintained its prognostic value when adjusted for the treatment of the patients.

RAN is a small GTP binding protein that belongs to the RAS superfamily and is required for the translocation of RNA and proteins through the nuclear pore complex, as well as the control of DNA synthesis and cell cycle progression^{42,43}. It is a member of the gene expression-based proliferation signature in which high expression was related to worse prognosis in MCL¹³. *MYC* is a transcription factor that plays a key role in cell cycle progression and apoptosis⁴⁴. Deregulation of *MYC* by mutation, overexpression or chromosomal rearrangements are common events in hematological malignancies⁴⁵. *MYC* has been found to be highly expressed in MCL^{46,47} and increased expression is associated with poor prognosis⁴¹. *TNFRSF10B* is a member of the TNF-receptor superfamily that triggers an apoptotic signal upon activation by the cytokine TRAIL. Inactivating mutations of *TNFRSF10B* have been found in different types of solid tumors and some types of non-Hodgkin's lymphomas⁴⁸. *POLE2* is the DNA polymerase epsilon B-subunit and, accordingly, is implicated in DNA replication, repair, recombination and cell cycle control functions^{49,50}. Like *RAN*, *POLE2* was also included in the array-based proliferation signature¹³. *SLC29A2* is a member of the SLC29 family of nucleoside carriers that transport a broad range of purine and pyrimidine nucleosides⁵¹. Interestingly, gene expression changes of this gene can affect the cellular uptake of nucleoside analogs in MCL cells and thus the therapeutic response to this group of anticancer agents^{32,52}.

An important feature of the proposed assay is its applicability to FFPE tumor tissue specimens. Nucleic acids from FFPE material are often degraded following the formalin fixation process⁵³. In addition, fixation chemically modifies the RNA structure in tumor tissues impeding subsequent analysis by molecular techniques such as quantitative RT-PCR⁵⁴. Nevertheless, numerous studies have demonstrated that mRNA from FFPE tissues can be extracted⁵⁵⁻⁵⁷ and analyzed by qRT-PCR^{19,58}. In our series, successful qRT-PCR analysis from mRNA derived from FFPE tissue strongly depended on short amplicon lengths (optimally up to 80 bp). Using optimized qRT-PCR assays we were able to amplify RNA from almost 75% of the archival samples examined. Importantly, the success rate among more recent cases collected as part of prospective clinical trials rose to 86% which is in the range of analyzable Ki-67 stainings in a recent study¹⁷. Although the five-gene model derived from the analysis of a large series of fresh frozen MCL specimens was clearly validated as a whole in the FFPE series, it should be noted that the performance of the qRT-PCR assays for *RAN* and *MYC* in FFPE tissue may need improvement before broader implementation in a routine setting or for guiding treatment decisions within future prospective clinical trials. Towards this goal, large cohorts of MCL patients from prospective clinical trials by the European Mantle

Cell Lymphoma Consortium will now be analyzed in order to validate the prognostic value of the proliferation signature in the context of current treatment approaches.

In summary, we developed a molecular test to predict survival in MCL patients at the time of diagnosis. This test is based on the quantitative measurement of the gene expression levels of five genes and can be applied to routinely obtained formalin-fixed and paraffin-embedded MCL tissue specimens. This test appears superior and more objective than the immunohistochemical measurement of the Ki-67 index and may be applied using an automated technical platform. Using this approach, large cohorts of MCL patients from prospective clinical trials will now be analyzed in order to validate the prognostic value of the proliferation signature in the context of current treatment approaches and, possibly, to make a step forward towards risk-adapted therapy in MCL patients.

REFERENCES

1. Fernandez V, Hartmann E, Ott G, et al: Pathogenesis of mantle-cell lymphoma: all oncogenic roads lead to dysregulation of cell cycle and DNA damage response pathways. *J Clin Oncol* 23:6364-9, 2005
2. Campo E, Raffeld M, Jaffe ES: Mantle-cell lymphoma. *Semin Hematol* 36:115-27, 1999
3. Bertoni F, Rinaldi A, Zucca E, et al: Update on the molecular biology of mantle cell lymphoma. *Hematol Oncol* 24:22-7, 2006
4. Swerdlow SH, Williams ME: From centrocytic to mantle cell lymphoma: a clinicopathologic and molecular review of 3 decades. *Hum Pathol* 33:7-20, 2002
5. Bernard M, Gressin R, Lefrere F, et al: Blastic variant of mantle cell lymphoma: a rare but highly aggressive subtype. *Leukemia* 15:1785-91, 2001
6. Bosch F, Lopez-Guillermo A, Campo E, et al: Mantle cell lymphoma: presenting features, response to therapy, and prognostic factors. *Cancer* 82:567-75, 1998
7. Greiner TC, Moynihan MJ, Chan WC, et al: p53 mutations in mantle cell lymphoma are associated with variant cytology and predict a poor prognosis. *Blood* 87:4302-10, 1996
8. Hernandez L, Fest T, Cazorla M, et al: p53 gene mutations and protein overexpression are associated with aggressive variants of mantle cell lymphomas. *Blood* 87:3351-9, 1996
9. Louie DC, Offit K, Jaslow R, et al: p53 overexpression as a marker of poor prognosis in mantle cell lymphomas with t(11;14)(q13;q32). *Blood* 86:2892-9, 1995
10. Salaverria I, Zettl A, Bea S, et al: Specific Secondary Genetic Alterations in Mantle Cell Lymphoma Provide Prognostic Information Independent of the Gene Expression-Based Proliferation Signature. *J Clin Oncol*, 2007
11. Rubio-Moscardo F, Climent J, Siebert R, et al: Mantle-cell lymphoma genotypes identified with CGH to BAC microarrays define a leukemic subgroup of disease and predict patient outcome. *Blood* 105:4445-54, 2005

12. Pinyol M, Bea S, Pla L, et al: Inactivation of RB1 in mantle cell lymphoma detected by nonsense-mediated mRNA decay pathway inhibition and microarray analysis. *Blood*, 2007
13. Rosenwald A, Wright G, Wiestner A, et al: The proliferation gene expression signature is a quantitative integrator of oncogenic events that predicts survival in mantle cell lymphoma. *Cancer Cell* 3:185-97, 2003
14. Tiemann M, Schrader C, Klapper W, et al: Histopathology, cell proliferation indices and clinical outcome in 304 patients with mantle cell lymphoma (MCL): a clinicopathological study from the European MCL Network. *Br J Haematol* 131:29-38, 2005
15. Katzenberger T, Petzoldt C, Holler S, et al: The Ki67 proliferation index is a quantitative indicator of clinical risk in mantle cell lymphoma. *Blood* 107:3407, 2006
16. Raty R, Franssila K, Joensuu H, et al: Ki-67 expression level, histological subtype, and the International Prognostic Index as outcome predictors in mantle cell lymphoma. *Eur J Haematol* 69:11-20, 2002
17. de Jong D, Rosenwald A, Chhanabhai M, et al: Immunohistochemical prognostic markers in diffuse large B-cell lymphoma: validation of tissue microarray as a prerequisite for broad clinical applications--a study from the Lunenburg Lymphoma Biomarker Consortium. *J Clin Oncol* 25:805-12, 2007
18. Jaffe E.S. HNL, Stein H., Vardiman J.W. (Eds.): World Health Organization Classification of Tumours. Pathology and Genetics of Tumours of Haematopoietic and Lymphoid Tissues. Lyon, IARC Press, 2001
19. Specht K, Richter T, Muller U, et al: Quantitative gene expression analysis in microdissected archival formalin-fixed and paraffin-embedded tumor tissue. *Am J Pathol* 158:419-29, 2001
20. Hernandez L, Bea S, Pinyol M, et al: CDK4 and MDM2 gene alterations mainly occur in highly proliferative and aggressive mantle cell lymphomas with wild-type INK4a/ARF locus. *Cancer Res* 65:2199-206, 2005
21. Pinyol M, Cobo F, Bea S, et al: p16(INK4a) gene inactivation by deletions, mutations, and hypermethylation is associated with transformed and aggressive variants of non-Hodgkin's lymphomas. *Blood* 91:2977-84, 1998
22. Bea S, Ribas M, Hernandez JM, et al: Increased number of chromosomal imbalances and high-level DNA amplifications in mantle cell lymphoma are associated with blastoid variants. *Blood* 93:4365-74, 1999
23. Bea S, Tort F, Pinyol M, et al: BMI-1 gene amplification and overexpression in hematological malignancies occur mainly in mantle cell lymphomas. *Cancer Res* 61:2409-12, 2001
24. Pinyol M, Hernandez L, Cazorla M, et al: Deletions and loss of expression of p16INK4a and p21Waf1 genes are associated with aggressive variants of mantle cell lymphomas. *Blood* 89:272-80, 1997
25. Cho-Vega JH, Rassidakis GZ, Admirand JH, et al: MCL-1 expression in B-cell non-Hodgkin's lymphomas. *Hum Pathol* 35:1095-100, 2004
26. Fernandez V, Jares P, Bea S, et al: Frequent polymorphic changes but not mutations of TRAIL receptors DR4 and DR5 in mantle cell lymphoma and other B-cell lymphoid neoplasms. *Haematologica* 89:1322-31, 2004
27. Khoury JD, Medeiros LJ, Rassidakis GZ, et al: Expression of Mcl-1 in mantle cell lymphoma is associated with high-grade morphology, a high proliferative state, and p53 overexpression. *J Pathol* 199:90-7, 2003
28. MacFarlane M, Kohlhaas SL, Sutcliffe MJ, et al: TRAIL receptor-selective mutants signal to apoptosis via TRAIL-R1 in primary lymphoid malignancies. *Cancer Res* 65:11265-70, 2005
29. Mestre-Escorihuela C, Rubio-Moscardo F, Richter JA, et al: Homozygous deletions localize novel tumor suppressor genes in B-cell lymphomas. *Blood* 109:271-80, 2007

30. Rubio-Moscardo F, Blesa D, Mestre C, et al: Characterization of 8p21.3 chromosomal deletions in B-cell lymphoma: TRAIL-R1 and TRAIL-R2 as candidate dosage-dependent tumor suppressor genes. *Blood* 106:3214-22, 2005
31. Tagawa H, Karnan S, Suzuki R, et al: Genome-wide array-based CGH for mantle cell lymphoma: identification of homozygous deletions of the proapoptotic gene BIM. *Oncogene* 24:1348-58, 2005
32. Marce S, Molina-Arcas M, Villamor N, et al: Expression of human equilibrative nucleoside transporter 1 (hENT1) and its correlation with gemcitabine uptake and cytotoxicity in mantle cell lymphoma. *Haematologica* 91:895-902, 2006
33. Bennaceur-Griscelli A, Bosq J, Koscielny S, et al: High level of glutathione-S-transferase pi expression in mantle cell lymphomas. *Clin Cancer Res* 10:3029-34, 2004
34. Thieblemont C, Nasser V, Felman P, et al: Small lymphocytic lymphoma, marginal zone B-cell lymphoma, and mantle cell lymphoma exhibit distinct gene-expression profiles allowing molecular diagnosis. *Blood* 103:2727-37, 2004
35. Livak KJ, Schmittgen TD: Analysis of relative gene expression data using real-time quantitative PCR and the 2(-Delta Delta C(T)) Method. *Methods* 25:402-8, 2001
36. Witzig TE: Current treatment approaches for mantle-cell lymphoma. *J Clin Oncol* 23:6409-14, 2005
37. Pinyol M, Hernandez L, Martinez A, et al: INK4a/ARF locus alterations in human non-Hodgkin's lymphomas mainly occur in tumors with wild-type p53 gene. *Am J Pathol* 156:1987-96, 2000
38. Moller MB, Nielsen O, Pedersen NT: Oncoprotein MDM2 overexpression is associated with poor prognosis in distinct non-Hodgkin's lymphoma entities. *Mod Pathol* 12:1010-6, 1999
39. Hartmann E FV, Stoecklein H, Hernández L, Campo E, Rosenwald A (in press): Increased MDM2 Expression is associated with inferior survival in Mantle Cell Lymphoma, but not related to the MDM2 SNP309. *Haematologica*, 2007
40. Wiestner A, Tehrani M, Chiorazzi M, et al: Point mutations and genomic deletions in Cyclin D1 create stable truncated mRNAs that are associated with increased proliferation rate and shorter survival in mantle cell lymphoma. *Blood*, 2007
41. Nagy B, Lundan T, Larramendy ML, et al: Abnormal expression of apoptosis-related genes in haematological malignancies: overexpression of MYC is poor prognostic sign in mantle cell lymphoma. *Br J Haematol* 120:434-41, 2003
42. Arnaoutov A, Dasso M: The Ran GTPase regulates kinetochore function. *Dev Cell* 5:99-111, 2003
43. Dasso M: The Ran GTPase: theme and variations. *Curr Biol* 12:R502-8, 2002
44. Liu J, Levens D: Making myc. *Curr Top Microbiol Immunol* 302:1-32, 2006
45. Janz S: Myc translocations in B cell and plasma cell neoplasms. *DNA Repair (Amst)* 5:1213-24, 2006
46. Hernandez L, Hernandez S, Bea S, et al: c-myc mRNA expression and genomic alterations in mantle cell lymphomas and other nodal non-Hodgkin's lymphomas. *Leukemia* 13:2087-93, 1999
47. Korz C, Pscherer A, Benner A, et al: Evidence for distinct pathomechanisms in B-cell chronic lymphocytic leukemia and mantle cell lymphoma by quantitative expression analysis of cell cycle and apoptosis-associated genes. *Blood* 99:4554-61, 2002
48. Lee SH, Shin MS, Kim HS, et al: Somatic mutations of TRAIL-receptor 1 and TRAIL-receptor 2 genes in non-Hodgkin's lymphoma. *Oncogene* 20:399-403, 2001
49. Burgers PM: Eukaryotic DNA polymerases in DNA replication and DNA repair. *Chromosoma* 107:218-27, 1998

50. Hubscher U, Nasheuer HP, Syvaaja JE: Eukaryotic DNA polymerases, a growing family. *Trends Biochem Sci* 25:143-7, 2000
51. Baldwin SA, Beal PR, Yao SY, et al: The equilibrative nucleoside transporter family, SLC29. *Pflugers Arch* 447:735-43, 2004
52. Molina-Arcas M, Marce S, Villamor N, et al: Equilibrative nucleoside transporter-2 (hENT2) protein expression correlates with ex vivo sensitivity to fludarabine in chronic lymphocytic leukemia (CLL) cells. *Leukemia* 19:64-8, 2005
53. Mizuno T, Nagamura H, Iwamoto KS, et al: RNA from decades-old archival tissue blocks for retrospective studies. *Diagn Mol Pathol* 7:202-8, 1998
54. Masuda N, Ohnishi T, Kawamoto S, et al: Analysis of chemical modification of RNA from formalin-fixed samples and optimization of molecular biology applications for such samples. *Nucleic Acids Res* 27:4436-43, 1999
55. Mies C: A simple, rapid method for isolating RNA from paraffin-embedded tissues for reverse transcription-polymerase chain reaction (RT-PCR). *J Histochem Cytochem* 42:811-3, 1994
56. Rupp GM, Locker J: Purification and analysis of RNA from paraffin-embedded tissues. *Biotechniques* 6:56-60, 1988
57. Stanta G, Bonin S: RNA quantitative analysis from fixed and paraffin-embedded tissues: membrane hybridization and capillary electrophoresis. *Biotechniques* 24:271-6, 1998
58. Cronin M, Pho M, Dutta D, et al: Measurement of gene expression in archival paraffin-embedded tissues: development and performance of a 92-gene reverse transcriptase-polymerase chain reaction assay. *Am J Pathol* 164:35-42, 2004

Supplementary Methods: *RNA extraction from FFPE material*

The present protocol was adapted from the method already described by Specht et al. (Specht K, Richter T, Muller U, et al, *Am J Pathol* 158:419-29, 2001). All centrifugations were carried for 5 minutes at maximum speed unless specified otherwise. All chemicals and solutions used were RNase-free. 5 to 10 cuts of 10-20 μm were obtained from each FFPE tumor specimen, and sealed in a sterile tube. Paraffin was removed by washing the tissue twice with 1 ml xylene, followed by centrifugation. The supernatant was discarded and the samples were rehydrated by three sequential washes with 100%, 90% and 75% ethanol, respectively, followed by centrifugation to collect the tissue. Afterwards, the tissue pellet was air-dried and resuspended in 200 μl of lysis buffer (10 mM Tris-HCl, pH8.0; 0.1 mM EDTA, pH 8.0; 2% SDS; pH 7.0) and 500 $\mu\text{g/ml}$ proteinase K (Roche Applied Science[®], Mannheim, Germany). Samples were incubated overnight in a thermomixer at 58°C and 1000rpm. The following day samples were centrifuged at 4 °C, and transferred to a new tube without taking any non-digested material. The RNA was purified by Phenol-Chloroform-extraction. The aqueous phase was transferred to a new tube, and 1 μl glycogen 20 mg/ml (Invitrogen[™], Carlsbad CA, USA), 1 μl Pellet Paint (optional) (Novagen[®], Darmstadt, Germany) and 500 μl isopropanol were added. The samples were precipitated at –20°C for 1-2 hours, followed by centrifugation for 20 minutes at 4°C. Finally, the pellets were washed with 75% ethanol, resuspended with DEPC water and quantified. The RNA samples were stored at –80°C until cDNA synthesis was started.

Table 1: *Clinical characteristics of the MCL patients.*

Characteristics of MCL cases	Frozen specimens	FFPE specimens
Median Age (years)	64	66
Sex		
Male	58 (80%)	31 (74%)
Female	15 (20%)	11 (26%)
Histology		
Typical	54 (74%)	35 (83%)
Blastoid	19 (26%)	7 (17%)
Median Survival (months)	34.5	36.3
Median Proliferation Index (Ki-67 staining)	30%	22%
Total number of cases	73	42

Abbreviations: MCL, mantle cell lymphoma; FFPE, formalin-fixed paraffin-embedded.

Table 2: Configuration of the Custom TaqMan® low-density array platform (Micro Fluidic Card).

Gene	Assay	Amplicon size (bp)	Function	Reference
ASPM	Hs00411505_m1	77	Proliferation	13
BCL2L11	Hs00708019_s1	92	Apoptosis	29,31
BMI1	Hs00180411_m1	105	Cell cycle	22,23
CCND1	Hs00277039_m1	94	Cell cycle	2
CDC2	Hs00176469_m1	101	Proliferation	13
CDC20 *	Hs00415851_g1	108	Proliferation	13
CDK4	Hs00175935_m1	65	Cell cycle	20
CDKN2A	Hs00233365_m1	117	Cell cycle	21,37
CDKN3 *	Hs00193192_m1	83	Proliferation	13
CEBPB	Hs00270923_s1	75	Proliferation	13
CENPF	Hs00193201_m1	99	Proliferation	13
DBF4	Hs00272696_m1	77	Proliferation	13
GSTP1	Hs00168310_m1	54	Metabolism	33,34
GTF2B	Hs00155315_m1	66	Proliferation	13
HMGB2 *	Hs00357789_g1	99	Proliferation	13
HPRT1 *	Hs99999909_m1	100	Proliferation	13
MCL1	Hs00172036_m1	124	Apoptosis	25,27
MCM2	Hs00170472_m1	82	Proliferation	13
MDM2	Hs00170472_m1	82	Cell cycle	20
MKI67 *	Hs00606991_m1	137	Proliferation	15
MYC *	Hs00153408_m1	107	Multiple	46,47
NEIL3	Hs00157387_m1	82	Proliferation	13
PCNA *	Hs00427154_g1	138	Proliferation	13
PIF1	Hs00228104_m1	104	Proliferation	13
POLE2 *	Hs00160277_m1	70	Proliferation	13
RAN *	Hs00741099_g1	146	Proliferation	13
SLC29A1	Hs00191940_m1	77	Nucleoside transport	32
SLC29A2	Hs00155426_m1	110	Nucleoside transport	32
TNFRSF10A	Hs00269491_m1	83	Apoptosis	26,28,30
TNFRSF10B	Hs00187196_m1	114	Apoptosis	26,28,30
TOP2A *	Hs00172154_m1	125	Proliferation	13

Gene	Assay	Amplicon size (bp)	Function	Reference
TUBA1B	Hs00744842_sH	110	Proliferation	¹³
UHRF1	Hs00273589_m1	105	Proliferation	¹³
18S	4342379	-	Control gene	-
B2M	Hs00187842_m1	64	Control gene	¹³

Abbreviations: bp, base pairs. Genes marked with an asterisk are significantly correlated with survival in univariate analysis.

Table 3: Predictive power of one- to five-gene models according to the C-index.

	Genes	C-Index
1-Gene-Model	<i>RAN</i>	0,690
2-Gene-Model	<i>RAN, MYC</i>	0,721
3-Gene-Model	<i>RAN, MYC, TNFRSF10B</i>	0,730
4-Gene-Model	<i>RAN, MYC, TNFRSF10B, POLE2</i>	0,754
5-Gene-Model	<i>RAN, MYC, TNFRSF10B, POLE2, SLC29A2</i>	0,762

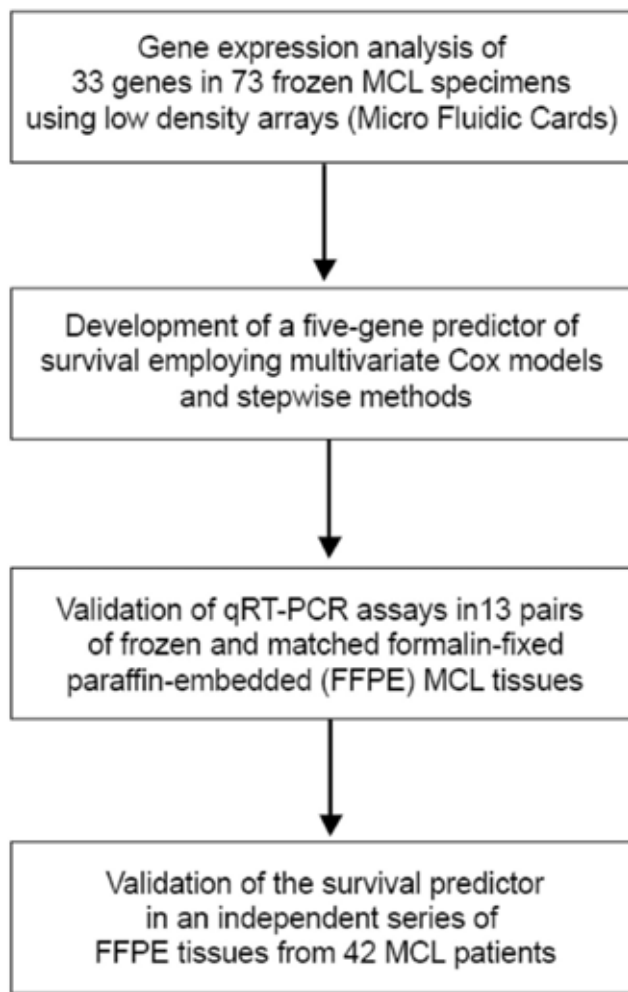
Figure 1: *Flow-chart describing the set-up of the study.*

Figure 2: C-index value according to the number of genes included in the survival predictor.

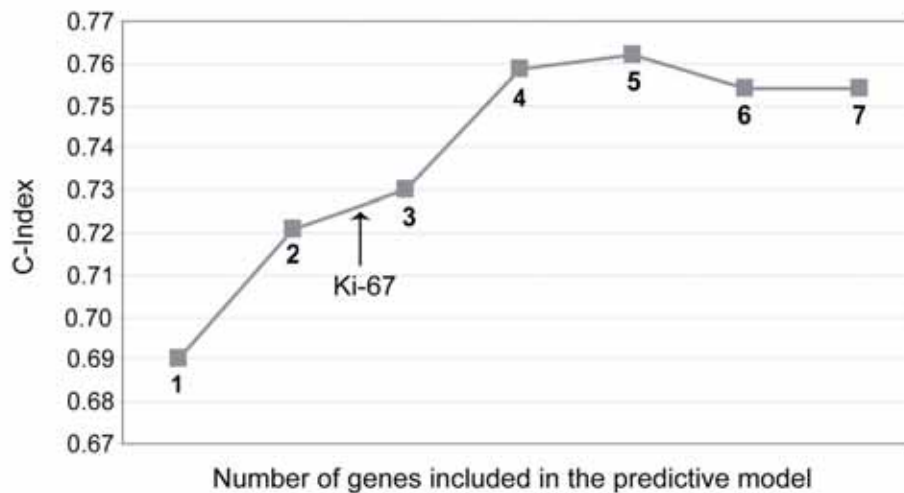
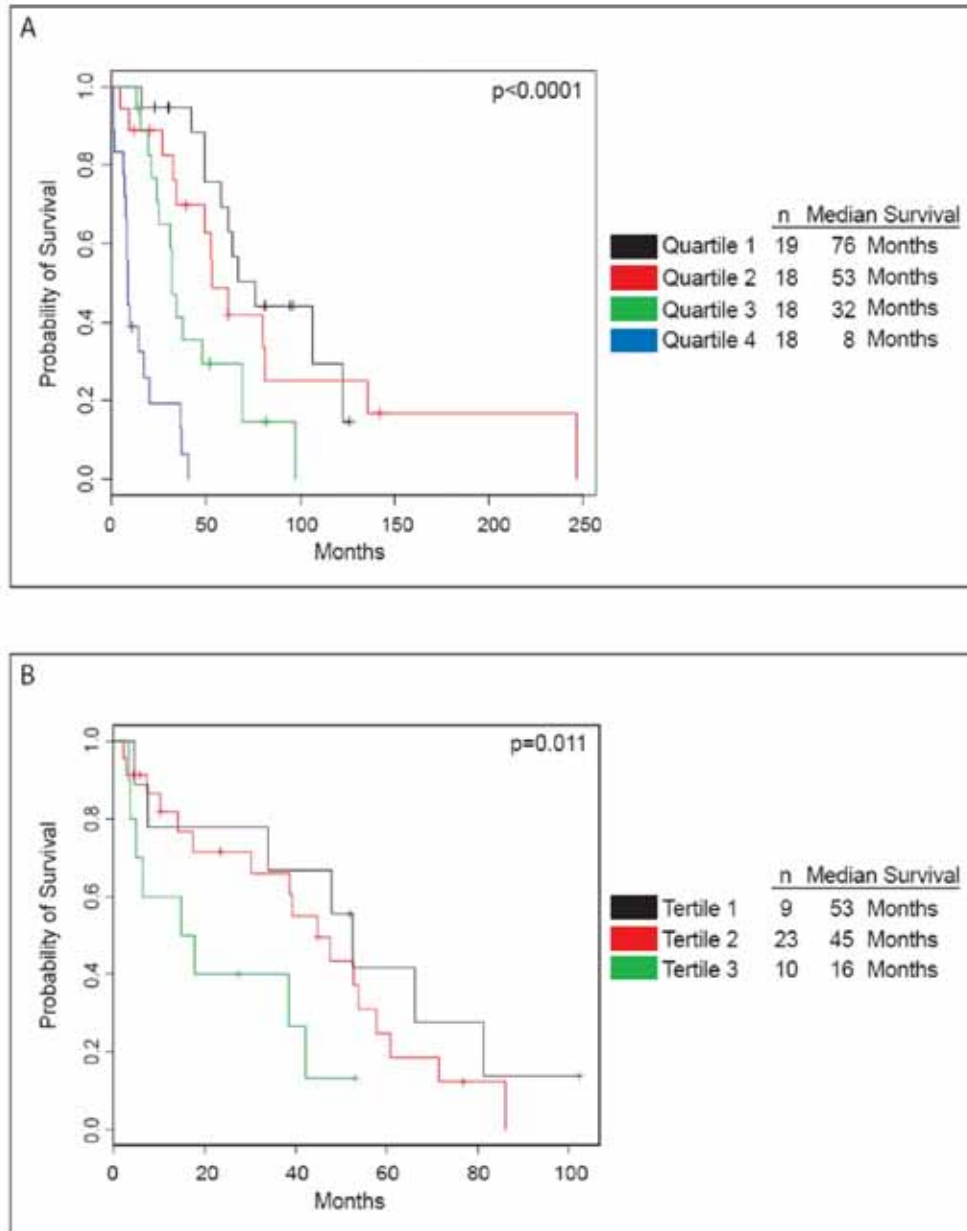


Figure 3: Kaplan-Meier plots visualizing survival groups according to the five-gene predictor in **A)** fresh frozen tumor samples from 73 MCL patients; and **B)** FFPE samples from 42 MCL patients.



Supplementary Table 1: *Clinical characteristics of the MCL patients*

MCL patient	Age (years)	Sex	Histology	Survival (months)	Status	Ki-67 (%)	Tissue
MCL1	63	M	blastoid	24	dead	40	frozen
MCL2	58	F	typical	52.5	dead	10	frozen
MCL3	74	M	blastoid	64.1	dead	30	frozen/FFPE
MCL4	n.a.	M	typical	69.4	dead	10	frozen
MCL5	63	M	typical	29.5	alive	10	frozen
MCL6	60	M	typical	81.3	dead	15	frozen
MCL7	39	M	typical	22.9	alive	20	frozen
MCL8	57	F	typical	80.1	dead	10	frozen
MCL9	50	M	typical	21.2	dead	n.a.	frozen
MCL10	61	M	typical	11.7	alive	10	frozen/FFPE
MCL11	59	M	typical	37.4	dead	30	frozen
MCL12	62	M	blastoid	16.8	dead	50	frozen
MCL13	51	F	typical	136	dead	20	frozen
MCL14	75	M	typical	67.1	dead	20	frozen
MCL15	69	F	blastoid	9.1	dead	50	frozen
MCL16	64	F	typical	48	dead	3	frozen
MCL17	n.a.	M	typical	122.4	dead	10	frozen
MCL18	70	M	typical	81.1	alive	30	frozen
MCL19	60	M	typical	10.6	alive	60	frozen/FFPE
MCL20	71	F	blastoid	20	dead	70	frozen
MCL21	51	M	typical	81.2	alive	10	frozen
MCL22	61	F	typical	32	dead	40	frozen
MCL23	71	F	typical	14	alive	40	frozen
MCL24	n.a.	F	typical	24.9	dead	50	frozen
MCL25	40	M	typical	96.4	alive	10	frozen
MCL26	67	M	typical	6.8	dead	60	frozen
MCL27	60	M	blastoid	97.4	dead	15	frozen/FFPE
MCL28	80	M	blastoid	40.6	dead	90	frozen
MCL29	58	M	typical	34	dead	100	frozen/FFPE
MCL30	52	M	typical	39.3	alive	30	frozen
MCL31	58	M	typical	14	dead	50	frozen/FFPE
MCL32	72	M	blastoid	1.6	dead	60	frozen/FFPE
MCL33	53	M	typical	7.8	dead	90	frozen/FFPE
MCL34	42	M	typical	81.6	alive	30	frozen
MCL35	70	M	typical	7.4	dead	20	frozen
MCL36	64	M	typical	69.4	dead	25	frozen/FFPE
MCL37	66	F	blastoid	1	dead	100	frozen
MCL38	64	M	typical	30.6	dead	25	frozen
MCL39	78	M	typical	4.7	dead	30	frozen/FFPE
MCL40	61	M	typical	106.3	dead	4	frozen/FFPE
MCL41	72	M	typical	49	dead	50	frozen
MCL42	61	M	typical	12.9	dead	40	frozen
MCL43	77	M	typical	30	alive	10	frozen
MCL44	64	F	blastoid	8.2	dead	60	frozen
MCL45	71	M	blastoid	42.5	dead	50	frozen

MCL patient	Age (years)	Sex	Histology	Survival (months)	Status	Ki67 (%)	Tissue
MCL46	51	M	blastoid	61.9	dead	5	frozen
MCL47	81	F	typical	6.3	dead	40	frozen/FFPE
MCL48	54	M	typical	19.5	dead	30	frozen
MCL49	85	M	blastoid	51.9	alive	20	frozen
MCL50	52	F	blastoid	49.1	dead	10	frozen
MCL51	67	M	blastoid	34.5	dead	30	frozen
MCL52	69	M	typical	32.6	dead	35	frozen
MCL53	78	M	typical	36.6	dead	30	frozen
MCL54	67	F	typical	26.5	dead	60	frozen
MCL55	81	M	blastoid	16	dead	10	frozen
MCL56	71	M	typical	53	dead	n.a.	frozen
MCL57	71	M	blastoid	37	dead	50	frozen
MCL58	37	M	typical	126.1	alive	30	frozen
MCL59	64	M	typical	49	dead	10	frozen
MCL60	82	M	typical	62	alive	30	frozen
MCL61	81	F	blastoid	8	dead	50	frozen
MCL62	75	M	blastoid	9.8	dead	70	frozen
MCL63	53	M	typical	20	alive	n.a.	frozen
MCL64	67	M	typical	142	alive	20	frozen
MCL65	67	M	typical	61.6	dead	20	frozen
MCL66	64	M	typical	76.2	dead	15	frozen
MCL67	67	M	typical	31.9	dead	15	frozen
MCL68	55	M	typical	15.3	dead	70	frozen
MCL69	61	M	typical	8.6	dead	70	frozen
MCL70	72	M	typical	58	dead	n.a.	frozen
MCL71	80	M	typical	1	dead	60	frozen
MCL72	40	M	typical	246.7	dead	20	frozen
MCL73	56	M	typical	94.2	alive	15	frozen/FFPE
MCL74	63	M	blastoid	10.3	alive	80	FFPE
MCL75	73	F	typical	52	alive	5	FFPE
MCL76	68	M	typical	14.2	dead	30	FFPE
MCL77	69	M	typical	10.2	dead	10	FFPE
MCL78	57	M	typical	102.5	alive	20	FFPE
MCL79	53	M	typical	53.1	alive	10	FFPE
MCL80	67	M	typical	57.7	dead	10	FFPE
MCL81	46	M	typical	14.9	dead	50	FFPE
MCL82	69	M	blastoid	7.5	dead	90	FFPE
MCL83	74	M	typical	3.7	dead	10	FFPE
MCL84	72	M	typical	7.3	dead	20	FFPE
MCL85	64	M	typical	77	alive	20	FFPE
MCL86	59	M	typical	47.6	dead	20	FFPE
MCL87	63	M	typical	66.3	dead	10	FFPE
MCL88	55	F	typical	52.5	dead	40	FFPE
MCL89	69	M	typical	38.6	dead	n.a.	FFPE
MCL90	52	F	typical	3.3	dead	40	FFPE
MCL91	77	F	typical	2.8	dead	40	FFPE
MCL92	69	M	typical	42.3	dead	40	FFPE
MCL93	64	M	blastoid	5	dead	70	FFPE

MCL patient	Age (years)	Sex	Histology	Survival (months)	Status	Ki67 (%)	Tissue
MCL94	54	M	blastoid	6.4	dead	90	FFPE
MCL95	73	F	blastoid	60.8	dead	40	FFPE
MCL96	40	M	typical	44.8	alive	30	FFPE
MCL97	71	M	typical	44.8	dead	20	FFPE
MCL98	64	M	typical	53.8	dead	n.a.	FFPE
MCL99	72	M	typical	5.8	alive	20	FFPE
MCL100	68	F	typical	86.2	dead	10	FFPE
MCL101	49	M	typical	81.3	dead	30	FFPE
MCL102	66	M	typical	17.5	dead	10	FFPE
MCL103	58	M	typical	71.6	dead	10	FFPE
MCL104	56	M	blastoid	52.7	dead	70	FFPE
MCL105	71	F	typical	47.9	dead	10	FFPE
MCL106	62	M	typical	39.4	dead	20	FFPE
MCL107	73	F	typical	38.7	dead	20	FFPE
MCL108	64	M	typical	17.8	dead	40	FFPE
MCL109	69	M	typical	27.5	alive	20	FFPE
MCL110	61	F	typical	34	dead	3	FFPE
MCL111	76	F	typical	4.3	alive	20	FFPE
MCL112	68	M	blastoid	2.2	dead	90	FFPE
MCL113	65	F	typical	23.5	alive	30	FFPE
MCL114	57	M	typical	30.3	dead	30	FFPE
MCL115	67	M	typical	4.6	dead	30	FFPE

Abbreviations: MCL, Mantle Cell Lymphoma; FFPE, Formalin-fixed, paraffin-embedded; F, female; M, male; n.a., not available

Supplementary Table 2: Expression data of the 5 genes included in the predictor for the MCL patients

MCL patient	RAN*	MYC*	TNFRSF10B*	POLE2*	SLC29A2*	Prognostic score ^{#&}
MCL1	2.06	-0.66	0.10	2.72	-0.92	3.10
MCL2	-0.30	0.26	-0.58	0.38	-2.00	-1.08
MCL3 [#]	0.83/-0.26	-1.74/1.19	-0.78/0.5	1.71/0.35	-2.08/1.65	-0.5/2.43
MCL4	1.45	1.08	0.73	-0.02	-0.02	1.76
MCL5	0.80	-0.79	0.18	0.73	-2.59	-2.03
MCL6	0.03	0.16	-0.55	0.28	-0.84	0.18
MCL7	0.92	-0.71	0.11	1.35	-1.68	-0.23
MCL8	0.80	-0.88	-0.26	1.32	0.16	1.66
MCL9	1.39	0.43	0.29	1.23	1.22	3.98
MCL10 [#]	0.04/0.00	0.33/1.07	-0.52/-0.94	1.03/-1.64	-2.17/0.07	-0.25/0.44
MCL11	0.96	-0.87	-0.90	2.07	-3.51	-0.45
MCL12	2.05	1.32	-0.15	2.61	-2.15	3.98
MCL13	0.59	0.16	0.24	1.76	-1.51	0.76
MCL14	-0.79	-1.32	1.61	2.05	1.18	-0.49
MCL15	0.69	-1.43	-0.93	1.35	-2.26	-0.72
MCL16	0.40	-0.18	-1.46	1.28	-1.50	1.46
MCL17	1.29	-0.63	0.31	1.40	-3.05	-1.30
MCL18	0.55	-2.06	-2.11	0.04	-4.88	-4.24
MCL19 [#]	0.89/-0.01	0.61/1.56	-0.65/0.11	2.79/0.75	0.55/1.60	5.49/3.79
MCL20	1.15	-0.72	-1.91	3.07	1.92	7.33
MCL21	0.90	-0.11	0.29	-0.50	-0.33	-0.33
MCL22	1.06	-0.33	-0.33	1.70	0.24	3.00
MCL23	1.10	-0.44	-0.51	1.07	-2.01	0.23
MCL24	1.20	0.54	-0.14	0.18	-0.01	2.05
MCL25	0.06	-0.38	0.05	-0.30	-2.25	-2.92
MCL26	0.91	0.00	-0.91	1.85	-0.90	2.77
MCL27 [#]	1.35/-0.23	-0.02/2.76	-0.32/0.15	2.47/0.47	-1.61/0.73	2.51/3.58
MCL28	1.36	0.17	-0.43	2.12	0.01	4.09
MCL29 [#]	0.62/0.02	-0.16/0.95	-0.78/-0.04	0.32/-0.02	-2.30/0.41	-0.74/1.40
MCL30	0.52	-1.19	-0.64	1.51	-1.16	0.32
MCL31 [#]	1.55/0.79	0.25/0.97	-1.25/-0.22	2.53/-0.14	-1.04/0.22	4.54/2.06
MCL32 [#]	2.08/0.38	1.62/2.14	0.71/0.54	2.45/0.43	0.69/1.67	6.13/4.08
MCL33 [#]	1.42/-0.31	2.58/2.82	-0.10/-0.41	2.24/0.02	0.51/1.47	6.85/4.41
MCL34	1.15	-0.49	-0.59	1.10	-1.46	0.89
MCL35	1.52	1.71	0.00	1.34	1.84	6.41
MCL36 [#]	0.97/-0.01	-0.19/2.47	-0.30/0.47	1.45/0.56	-0.10/1.81	2.43/4.36
MCL37	0.87	0.64	-0.63	1.89	-1.44	2.59
MCL38	1.32	-0.44	0.09	2.10	-2.35	0.54
MCL39 [#]	1.06/0.30	-0.77/-0.21	0.03/0.24	1.86/0.18	-1.43/0.60	0.69/0.63
MCL40 [#]	0.62/1.24	0.18/4.12	0.32/1.43	1.13/0.38	-3.22/-0.29	-1.61/4.02
MCL41	1.78	-1.42	-0.68	1.65	-2.87	-0.18
MCL42	1.15	0.53	-0.24	1.26	-0.74	2.44
MCL43	0.17	-1.85	-0.82	0.60	-2.43	-2.69
MCL44	1.39	1.10	-0.88	1.52	0.17	5.06
MCL45	0.17	-1.12	-0.44	1.97	-3.52	-2.06

MCL patient	RAN*	MYC*	TNFRSF10B*	POLE2*	SLC29A2*	Prognostic score^{#&}
MCL46	-0.49	-2.03	-1.08	-0.50	-3.11	-5.05
MCL47 [#]	1.68/1.07	1.20/3.26	0.22/0.32	3.33/1.31	0.88/1.51	6.87/6.83
MCL48	1.62	-0.41	0.44	3.23	-1.44	2.56
MCL49	1.55	-1.09	-0.39	2.12	0.18	3.15
MCL50	-1.30	0.81	0.32	-0.61	3.05	1.63
MCL51	1.22	-1.26	-0.87	2.36	0.34	3.53
MCL52	0.50	-1.01	-0.92	2.17	-2.56	0.02
MCL53	1.72	-0.80	-1.25	2.74	-4.00	0.91
MCL54	0.22	-0.16	-0.76	0.15	-1.26	-0.29
MCL55	0.58	-1.67	-0.71	1.12	-2.87	-2.13
MCL56	0.41	-1.06	-0.68	1.48	-2.23	-0.72
MCL57	1.47	0.34	-0.69	2.17	-3.01	1.66
MCL58	-1.61	-0.60	1.10	2.64	2.46	1.79
MCL59	1.26	-1.57	-0.88	1.20	-4.02	-2.25
MCL60	0.14	0.57	-0.98	-0.30	-3.53	-2.14
MCL61	1.95	1.83	-0.23	2.43	0.56	7.00
MCL62	1.46	1.66	1.06	2.86	-1.28	3.64
MCL63	0.52	-1.73	-1.54	1.57	-3.13	-1.23
MCL64	1.02	-0.22	-0.09	1.82	-3.19	-0.48
MCL65	-1.10	0.60	0.62	2.13	1.48	2.49
MCL66	0.34	-1.01	-0.36	0.92	-2.06	-1.45
MCL67	2.08	-0.72	0.90	3.18	-1.16	2.48
MCL68	1.78	-0.44	0.70	2.38	0.65	3.67
MCL69	1.55	1.45	-0.77	2.11	-0.64	5.24
MCL70	0.75	-1.46	-0.93	1.29	-3.53	-2.02
MCL71	1.11	-0.35	-1.43	2.09	-0.50	3.78
MCL72	0.25	-0.10	0.74	2.20	1.08	2.69
MCL73 [#]	0.48/-0.60	-1.04/0.09	0.31/0.75	0.87/-0.81	-1.78/0.54	-1.78/-1.53
MCL74	1.74	-0.46	1.07	0.39	0.00	0.60
MCL75	0.56	0.05	1.46	-1.14	-1.07	-3.06
MCL76	0.89	0.43	1.01	-1.24	2.09	1.16
MCL77	0.35	1.96	1.61	-0.64	0.59	0.65
MCL78	2.01	1.16	2.45	-1.56	-1.49	-2.33
MCL79	2.86	3.26	2.77	-0.61	2.36	5.10
MCL80	0.08	2.47	2.46	-1.30	2.49	1.28
MCL81	1.86	2.88	-0.77	0.68	2.16	8.35
MCL82	0.86	1.87	0.01	-0.29	-3.43	-1.00
MCL83	2.14	1.07	2.97	0.72	3.18	4.14
MCL84	3.24	-0.13	1.05	0.46	0.62	3.14
MCL85	0.49	0.70	1.60	-0.04	1.26	0.81
MCL86	0.50	-2.12	-1.46	-0.12	1.31	1.03
MCL87	0.71	-0.76	0.47	-1.01	1.39	-0.14
MCL88	-0.03	-0.82	1.38	0.71	1.21	-0.31
MCL89	2.82	3.27	3.23	0.09	3.94	6.89
MCL90	1.28	4.46	0.42	1.10	3.22	9.64
MCL91	-0.27	1.27	2.14	-1.02	2.27	0.11
MCL92	3.51	1.46	3.03	0.89	3.19	6.02
MCL93	0.74	3.40	1.34	-0.20	2.40	5.00

MCL patient	RAN*	MYC*	TNFRSF10B*	POLE2*	SLC29A2	Prognostic score^{#&}
MCL94	2.43	3.74	2.08	-0.20	0.93	4.82
MCL95	0.60	1.73	0.85	0.36	1.39	3.23
MCL96	1.16	0.13	1.21	-0.68	0.82	0.22
MCL97	0.55	2.69	1.30	0.12	0.45	2.51
MCL98	0.11	1.56	0.56	-0.27	1.13	1.97
MCL99	-0.11	1.92	0.32	-1.04	2.06	2.51
MCL100	-0.24	1.42	0.65	-0.89	1.47	1.11
MCL101	-0.35	1.23	0.45	-0.42	-0.15	-0.14
MCL102	1.45	1.65	1.11	-0.61	0.53	1.91
MCL103	1.53	2.07	1.77	0.58	1.26	3.67
MCL104	0.15	1.53	-1.63	1.74	-1.83	3.22
MCL105	0.10	-2.42	-0.56	-1.15	-0.64	-3.55
MCL106	2.36	-0.18	0.43	0.48	0.61	2.84
MCL107	0.38	1.73	0.96	0.59	2.13	3.87
MCL108	0.42	3.2	-0.27	0.77	2.82	7.48
MCL109	-0.53	3.48	0.66	2.09	1.35	5.73
MCL110	0.68	0.03	0.36	-1.28	-0.41	-1.34
MCL111	0.30	0.64	0.26	0.43	-0.76	0.35
MCL112	0.05	2.14	0.68	0.13	1.02	2.66
MCL113	0.62	1.91	1.51	-0.59	2.15	2.58
MCL114	0.20	2.08	0.32	-0.53	2.34	3.77
MCL115	-0.20	-0.25	0.05	-0.61	0.52	-0.59

* :- $\Delta\Delta\text{CT}$ value calculated according B2M control gene

:Value from frozen material (Micro Fluidic cards)/ Value from FFPE

&: Sum of the expression data for the given genes, reversing the sign for TNFRSF10B.

L'augment de l'expressió de MDM2 s'associa amb menor supervivència en el limfoma de cèl·lules del mantell, però no es relaciona amb la presència del SNP309

En aquest treball s'ha vist que l'augment de l'expressió del gen MDM2, un regulador negatiu de p53, correlaciona amb una menor supervivència en una sèrie de 43 limfomes de cèl·lules del mantell. La sobreexpressió de MDM2 s'associa amb guanys del nombre de còpies de dit gen però no amb la presència del polimorfisme SNP309, localitzat al promotor de MDM2.

* La contribució personal en aquest treball ha estat la participació en el disseny experimental del projecte, l'extracció de material genètic de les mostres (DNA i RNA) i posterior anàlisi del locus genòmic i de l'expressió del gen MDM2 mitjançant la tecnologia de la PCR quantitativa a temps real (qPCR); així com la determinació de l'estat mutacional del gen p53, la interpretació dels resultats i anàlisi de dades, i la redacció del treball.

Letters to the Editor

Increased MDM2 expression is associated with inferior survival in mantle cell lymphoma, but not related to the MDM2 SNP309

We here show that increased expression of MDM2, a negative regulator of p53, correlates with inferior survival in a series of 43 mantle cell lymphomas. MDM2 overexpression is associated with copy number gains of the MDM2 locus in single tumors, but not with the recently reported MDM2 promoter SNP309.

Hematologia 2007; 92:574-575

Mantle-cell lymphoma (MCL), a subtype of B-cell non-Hodgkin's lymphomas (B-NHL), is usually associated with poor clinical outcome. The genetic hallmark of MCL is the translocation t(11;14)(q13;32), resulting in overexpression of cyclin D1 and deregulation of the cell cycle. The DNA damage response pathway is also frequently affected by genetic alterations, e.g. by impairment of the ATM and p53 genes.¹ Other members of this pathway are less well studied, such as MDM2. MDM2 acts as a central negative regulator of p53, and is considered to be an oncogene.² MDM2 overexpression is associated with tumor progression and predicts decreased survival in solid tumors and hematological malignancies.^{3,4} In MCL, a subset of cases shows increased levels of MDM2 expression, but only single cases harbor genomic gains or amplifications of the MDM2 locus.⁵ Thus, the increased MDM2 expression often remains unexplained. Recently, a single nucleotide polymorphism (SNP) in the MDM2 promoter (T309G) was found to increase the affinity of the transcription factor Sp1, leading to enhanced expression of MDM2.⁶ Several reports have linked the presence of this SNP to an increased risk and/or earlier onset of malignant tumors.⁷

In the present study we investigated the MDM2 gene expression levels of 43 MCL samples in relationship to clinical outcome, genomic status of MDM2 and presence of MDM2 SNP309. Frozen tumor samples were obtained from the Institute of Pathology, University of Würzburg and the Hospital Clinic, University of Barcelona. Thirty-two cases showed typical and 11 blastoid morphology. The proliferation fraction was evaluated by Ki-67 staining as previously described.⁸ RNA and DNA were isolated according to standard protocols. MDM2 gene expression levels were determined by TaqmanTM Real-time quantitative RT-PCR with pre-developed assays (Applied Biosystems, MDM2: Hs_00234753_m1, B2M: Hs_00187842_m1) and calculated with the 2- $\Delta\Delta$ Ct method using B2M as endogenous control. MDM2 genomic status was assessed using a quantitative PCR approach as previously described.⁹ The MDM2 SNP309 was examined by direct sequencing, as described⁶ and validated by subcloning into the pCR2.1TA cloning vector (Invitrogen) and sequencing. The mutational status of p53 was studied by sequencing (36 cases) as reported.⁸ The association between MDM2 gene expression and survival was determined with the Cox hazard regression model. μ values for the associations between continuous and qualitative variables were calculated using an analysis of variance test. The χ^2 test was applied to analyze categorical data. p values <0.05 were considered significant.

The median survival of MCL patients in our series was 48 months. MDM2 gene expression was highly variable, showing a 14-fold range between the cases with highest

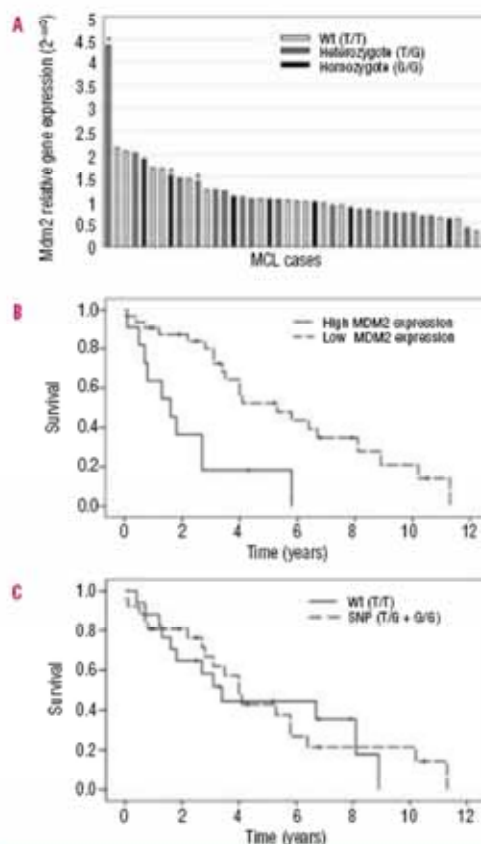


Figure 1. A. MDM2 gene expression levels in 43 MCL cases measured by real-time quantitative RT-PCR. Expression levels were calculated with the relative 2^{-ΔΔCt} method, using B2M as an endogenous control. Different bar colors depict the status of the SNP309 in the MDM2 promoter. Samples with a genomic copy number gain of the MDM2 locus are marked with an asterisk. Kaplan-Meier plots visualizing survival groups according to B. MDM2 mRNA expression (cutoff >75% percentile), and C. SNP309 status.

and lowest expression (Figure 1A). Importantly, increased expression was associated with poor prognosis in this series ($p=0.006$, Figure 1B). On the genomic level, three MCL cases showed evidence of an allelic gain of the MDM2 locus, correlating with increased MDM2 expression ($p=0.005$). However, increased MDM2 expression was present in many additional MCL tumors which did not harbor chromosomal gains in the MDM2 locus (Figure 1A). Since MDM2 gene expression levels are influenced by the MDM2 SNP309, we studied its potential impact on MDM2 expression in our series of MCL. The observed MDM2 SNP309 frequencies correlated well with the frequencies reported in a healthy population⁸ (Table 1). The presence of the SNP309 was not related to MDM2 mRNA expression (Figure 1C; $p=0.74$), age at diagnosis, morphological subtype and Ki-67 index. Likewise, there was no correlation between the presence of the SNP309 and survival. Interestingly, the G allele of SNP309 was observed in 9 out of ten female patients (Table 1; $p=0.029$). Several studies suggest that the MDM2 SNP309 may accelerate tumor formation in a

Table 1. Summary of the MDM2 SNP309 status in 43 MCL cases and association with age at diagnosis, sex, histology, proliferation fraction (Ki-67) and p53 status (wt: wild-type; mut: p53 mutation).

SNP status	Frequency (cases, %)	Age at diagnosis (years)	Sex		Histology		Ki67 (%)	P53	
			Male	Female	Common	Blasticoid		Wt	mut
Wildtype (T/T)	17 (39.5%)	64.1	16	1	14	3	35	12	2
Heterozygot (T/G)	19 (44.2%)	63.2	12	7	14	5	35	10	5
Homozygot (G/G)	7 (16.4%)	63.7	5	2	4	3	32	6	1
G allele (T/G+G/G)	26 (60.5%)	63.3	17	9	18	8	34	16	6
Total			33	10	32	11		28	8

gender and hormone specific way in women.⁷ In MCL, the presence of the G allele in women showed no association with younger age of tumor onset or survival when compared to men. 36 MCL cases were further analyzed for the p53 status, and 8 of them showed p53 mutations. As previously described¹⁰, p53 mutations were found to be associated with poor prognosis in our series ($p=0.036$). However, no correlation between the presence of the MDM2 SNP309 or MDM2 mRNA expression and p53 status was observed.

In conclusion, we provide evidence that besides p53 alterations, increased gene expression levels of MDM2 are directly correlated with inferior survival in MCL patients, underlining the importance of the DNA damage response pathway for the pathogenesis of MCL. In single MCL tumors, genomic gains of the MDM2 locus probably account for elevated MDM2 expression levels, while the presence of the SNP309 has no impact.

Elena Hartmann,* Verónica Fernández,° Heike Szecklein,* Luis Hernández,° Elias Campo,° Andreas Rosenwald*

*Institute of Pathology, University of Würzburg, Germany; °Hematopathology Section, Department of Pathology, Hospital Clinic, University of Barcelona, Spain

EH and VF contributed equally to this work; EC and AR are co-senior authors of this study.

Funding: supported by the Interdisciplinary Center for Clinical Research (IZKF), University of Würzburg (A.R.), the European Grant No. 503351 (European Mantle Cell Lymphoma Network, A.R., E.C.), the Lymphoma Research Foundation (LRF), USA (A.R., E.C.) and the grant CICYT SAF 05/5855 by the Spanish Ministry of Science (E.C.). Verónica Fernández is a recipient of a predoctoral fellowship from the Spanish Ministry of Education and Science (MEC).

Acknowledgments: we thank Inge Klier for her excellent technical assistance.

Key words: mantle cell lymphoma, MDM2 expression, survival, SNP309

Correspondence: Andreas Rosenwald, M.D., Institute of Pathology, University of Würzburg, Josef-Schneider-Str. 2, 97080 Würzburg, Germany. E-mail: rosenwald@mail.uni-wuerzburg.de

References

- Fernandez V, Hartmann E, Ott G, Campo E, Rosenwald A. Pathogenesis of mantle-cell lymphoma: all oncogenic roads lead to dysregulation of cell cycle and DNA damage response pathways. *J Clin Oncol* 2005; 23:6364-9.
- Brooks CL, Gu W. p53 ubiquitination: Mdm2 and beyond. *Mol Cell* 2006; 21:307-15.
- Turbin DA, Cheang MC, Bajdik CD, Gelmon KA, Yorlida E, De Luca A, et al. MDM2 protein expression is a negative prognostic marker in breast carcinoma. *Mod Pathol* 2006; 19:69-74.
- Møller MB, Nielsen O, Pederzen NT. Oncoprotein MDM2 overexpression is associated with poor prognosis in distinct non-Hodgkin's lymphoma entities. *Mod Pathol* 1999; 12:1010-6.
- Hernandez L, Bea S, Pinyol M, Ott G, Katzenberger T, Rosenwald A, et al. CDK4 and MDM2 gene alterations mainly occur in highly proliferative and aggressive mantle cell lymphomas with wild-type INK4a/ARF locus. *Cancer Res* 2005; 65:2199-206.
- Bond GL, Hu W, Bond EE, Robins H, Lutzker SG, Arva NC, et al. A single nucleotide polymorphism in the MDM2 promoter attenuates the p53 tumor suppressor pathway and accelerates tumor formation in humans. *Cell* 2004; 119:591-602.
- Bond GL, Himshfield KM, Kirchhoff T, Alexe G, Bond EE, Robins H, et al. MDM2 SNP309 accelerates tumor formation in a gender-specific and hormone-dependent manner. *Cancer Res* 2006; 66:5104-10.
- Katzenberger T, Petzoldt C, Holler S, Mader U, Kalla J, Adam P, et al. The Ki67 proliferation index is a quantitative indicator of clinical risk in mantle cell lymphoma. *Blood* 2006; 107:3407.
- Pinyol M, Hernandez L, Martinez A, Cobo F, Hernandez S, Bea S, et al. INK4a/ARF locus alterations in human non-Hodgkin's lymphomas mainly occur in tumors with wild-type p53 gene. *Am J Pathol* 2000; 156:1987-96.
- Greiner TC, Moynihan MJ, Chan WC, Lytle DM, Pedersen A, Anderson JR, et al. p53 mutations in mantle cell lymphoma are associated with variant cytology and predict a poor prognosis. *Blood* 1996; 87:4302-10.

TREBALL 2: APOPTOSI EN NHL

**Els canvis polimòrfics però no els mutacionals dels receptors de TRAIL
DR4 i DR5 són freqüents en el limfoma de cèl·lules del mantell i altres
neoplàsies limfoides de cèl·lula B**

Haematologica, 2004 (89): 1322-1331

(Journal impact factor 2006: 5.032)

Els canvis polimòrfics però no els mutacionals dels receptors de TRAIL DR4 i DR5 són freqüents en el limfoma de cèl·lules del mantell i altres neoplàsies limfoides de cèl·lula B

Els receptors de TRAIL DR4 (TNFRSF10A) i DR5 (TNFRSF10B) es localitzen a la regió cromosòmica 8p21-22, una zona freqüentment delecionada en diferents neoplàsies limfoides. S'ha examinat la presència d'alteracions en els exons 3, 4 i 9 d'aquests gens en un grup de neoplàsies limfoides, concretament 69 MCL, 16 CLL, 12 FL, 17 DLBCL i 4 línies cel·lulars que tenen la translocació t(11;14); així com en 91 donants de sang normals. Tres CLL i tres MCL tenien delecions de 8p. Només es van trobar dos canvis nucleotídics, situats a dins o al llindar de la seqüència consens acceptora d'*splicing* de l'intró 3 en dos MCL; i un canvi silenciós en una CLL. Aquests canvis també es trobaven a la línia germinal dels pacients. A més al domini de mort del gen DR4 (TNFRSF10A), el polimorfisme A1322G es va trobar associat significativament al risc a patir MCL [*odds ratio* (OR) = 5.9; 95% interval de confiança (CI), 1.92-18.1] i CLL (OR = 4.5; CI, 1.18-17), comparat amb una població normal ajustada per edat i sexe. Per altra banda, el polimorfisme C626G de l'exó 4 del gen de DR4 (TNFRSF10A) s'associa significativament amb una disminució del risc a patir MCL (OR = 0.3; CI, 0.12-0.8). No es van trobar mutacions ni canvis polimòrfics en els dominis del gen DR5 (TNFRSF10B). Aquestes troballes indiquen que les mutacions dels gens DR4 (TNFRSF10A) i DR5 (TNFRSF10B) són poc freqüents en neoplàsies limfoides però que els polimorfismes de DR4 (TNFRSF10A) poden contribuir a la patogènesi d'aquests tumors.

* La contribució personal en aquest treball ha estat la detecció de mutacions i polimorfismes en els dominis d'unió a lligand i de mort dels gens DR4 (TNFRSF10A) i DR5 (TNFRSF10B) en mostres tumorals i normals, mitjançant la reacció en cadena de la polimerasa (PCR), la cromatografia líquida desnaturalitzant d'alt rendiment (DHPLC) i tècniques de seqüenciació directa. També s'ha participat en la interpretació dels resultats, l'anàlisi de dades, i la redacció del treball.



[haematologica]
2004;89:1322-1331

VERÓNICA FERNÁNDEZ
PEDRO JARES
SILVIA BEA
ITZIAR SALAVERRIA
ELISABET GUINO
SILVIA DE SANJOSE
DOLORS COLOMER
GERMAN OTT
EMILI MONTSERRAT
ELIAS CAMPO

Malignant Lymphomas • Research Paper

Frequent polymorphic changes but not mutations of TRAIL receptors DR4 and DR5 in mantle cell lymphoma and other B-cell lymphoid neoplasms

A B S T R A C T

Background and Objectives. Tumor necrosis factor related apoptosis-inducing ligand (TRAIL) receptors DR4 and DR5 have been mapped to chromosome 8p21-22, a region frequently deleted in different lymphoid neoplasms.

Design and Methods. To investigate the potential alterations of these genes in lymphoid neoplasms, we examined the presence of gene mutations in exons 3, 4, and 9 in 69 cases with mantle cell lymphoma (MCL), 16 with chronic lymphocytic leukemia (CLL), 12 with follicular lymphomas (FL) and 17 with large B-cell-lymphomas (DLBCL), as well as in 4 lymphoid cell lines carrying the t(11;14) translocation, and 91 healthy blood donors.

Results. Three CLL and three MCL cases had 8p deletions. Two nucleotide changes in or near the intron 3 splice consensus sequence and a silent change were found. These rare changes were also present in the germ-line of the patients. The DR4 death domain A1322G polymorphism was significantly more frequent in MCL [odds ratio (OR) = 5.9; 95% confidence interval (CI), 1.92-18.1] and CLL (OR = 4.5; CI, 1.18-17) patients than in a sex and age-adjusted healthy population. In contrast, the DR4 exon 4 C626G polymorphism was associated with a significant overall decreased risk for MCL (OR = 0.3; CI, 0.12-0.8). No mutations or cancer-associated polymorphic changes were found in DR5 domains.

Interpretation and Conclusions. These findings indicate that mutations of DR4 and DR5 are uncommon in lymphoid neoplasms but DR4 polymorphic alleles may contribute to the pathogenesis of these malignancies.

Key words: TRAIL receptors, mantle cell lymphoma, DR4, DR5, polymorphisms.

From the Hematopathology Section, Laboratory of Pathology (VF, SB, IS, DC, EC), Genomics Unit (PJ), and Hematology Department, Hospital Clinic, Institut d'Investigacions Biomediques August Pi i Sunyer (IDIBAPS), University of Barcelona, Barcelona, Spain (EM), Epidemiology and Cancer Register Service, Institut Català d'Oncologia (EG, SdS); Institute of Pathology, University of Würzburg, Würzburg, Germany (GO).

Correspondence:
Elias Campo,
Laboratory of Pathology,
Hospital Clinic, Villarroel 170,
08038-Barcelona, Spain.
E-mail: ecampo@clinic.ub.es

©2004, Ferrata Storti Foundation

The tumor necrosis factor related apoptosis-inducing ligand (TRAIL) is a cytokine involved in the modulation of cell survival in different cell models.¹⁻⁴ Similarly to other tumor necrosis factor (TNF) family members, TRAIL mediates apoptosis by binding to two receptors, DR4 and DR5, with a common structural organization characterized by an extracellular cysteine-rich domain required for ligand binding and an intracellular death domain essential for the apoptotic signal transduction.⁷⁻¹³ Like the homologous FAS, TRAIL receptors seem to participate in the regulation of different lymphoid cell populations, in particular by preventing the expansion of autoreactive lymphocytes and the development of autoimmune disorders. Inactivation of the coding for these receptors may interfere with the normal mechanisms of cell survival facilitating the accumulation of abnormal lymphoid cell clones and eventually the development of lymphoid neoplasms. Apoptosis-related TNF receptors have been found to be inactivated in several human neoplasms and cancer cell lines. Germ-line mutations of FAS cause an autoimmune lymphoproliferative syndrome and an increased risk of lymphoid malignancies.^{14,15} In addition, somatic mutations of FAS have been detected in human tumors, including lymphoid neoplasms.¹⁶ Similarly, mutations of the DR4 and DR5 TRAIL receptors have been found in different types of solid tumors and occasional cases of non-Hodgkin's lymphoma (NHL).²¹⁻²³ Most of these mutations occur in the functional death and ligand binding domains and changes in other regions of the receptors are extremely rare. In addition to somatic mutations, several polymorphisms of regulatory regions or functional domains of FAS and TRAIL receptors have been frequently asso-

ciated with the development of lymphoid neoplasms. Apoptosis-related TNF receptors have been found to be inactivated in several human neoplasms and cancer cell lines. Germ-line mutations of FAS cause an autoimmune lymphoproliferative syndrome and an increased risk of lymphoid malignancies.^{14,15} In addition, somatic mutations of FAS have been detected in human tumors, including lymphoid neoplasms.¹⁶ Similarly, mutations of the DR4 and DR5 TRAIL receptors have been found in different types of solid tumors and occasional cases of non-Hodgkin's lymphoma (NHL).²¹⁻²³ Most of these mutations occur in the functional death and ligand binding domains and changes in other regions of the receptors are extremely rare. In addition to somatic mutations, several polymorphisms of regulatory regions or functional domains of FAS and TRAIL receptors have been frequently asso-

DR4 and DR5 in mantle cell lymphoma

ciated with different types of human tumors.^{6,19,21} Some of these polymorphic variants seem to impair the normal functional mechanism of the receptors and may facilitate the development or expansion of aberrant cell clones. Thus, polymorphic changes in the FAS promoter region have been associated with cervical squamous cell carcinoma and acute myeloid leukemia, whereas increased frequencies of several polymorphisms of the TRAIL receptor DR4 death and ligand domains have been detected in human ovarian, bladder, lung, head and neck, and gastric carcinomas, suggesting that these polymorphic variants may be associated with a predisposition to common malignancies.^{6,23-26}

Mantle cell lymphoma (MCL) is an aggressive lymphoid neoplasm characterized by the t(11;14) translocation with deregulation of the cyclin D1 gene.²⁶ The response of this tumor to conventional chemotherapeutic treatments is particularly poor with frequent relapses and short survival. The reasons for this drug resistance are not well known. TRAIL receptors DR4 and DR5 have been mapped to chromosome 8p21-22,^{27,28} a region frequently lost in MCL (7-57%) and chronic lymphocytic leukemia (CLL) (7%).^{29,30} Interestingly, 8p deletions have been associated with clinical progression and cell transformation in CLL, a lymphoid neoplasm in which failure of apoptotic mechanisms seems to play a crucial pathogenic role.³¹ To determine the potential role of inactivation of DR4 and DR5 TRAIL receptors in MCL and other lymphoid neoplasms we examined the presence of mutations and polymorphic variants in the ligand binding and death domains of these genes in a large series of patients with tumors and in the healthy population.

Design and Methods

Case selection

Tumor specimens from 114 patients with non-Hodgkin's lymphoid neoplasms were obtained from the Department of Pathology of the Hospital Clinic, University of Barcelona, and the Department of Pathology, University of Würzburg, on the basis of the availability of frozen samples for molecular studies. The patients had given their informed consent and the study was approved by the hospital review board. The types of tumor were MCL (n=69), CLL (n=16), follicular lymphoma (FL) (n=12), and diffuse large B-cell lymphomas (DLBCL) (n=17). Twenty-eight tumors had been analyzed by comparative genomic hybridization (CGH), and 3 cases each of CLL and MCL showed losses of chromosome 8p region. We also studied REC-1, Granta-519, JVM-2, and NCEB-1 cell lines carrying the t(11;14) translocation and samples from 91 healthy randomly selected blood donors. Data on age and sex were available for all included subjects.

DNA extraction and polymerase chain reaction

High molecular weight DNA was extracted from frozen samples using the standard proteinase K/RNase treatment and phenol-chloroform extraction. DNA from samples from the healthy blood donors was extracted using the Qiagen DNA extraction kit (Qiagen, GmbH, Germany). DNA from normal tissues or granulocytes from a subset of patients was extracted to examine whether the changes detected in the tumor DNA were present in the germ-line. Polymerase chain reaction (PCR) was performed in a total volume of 50 µL using 100 ng genomic DNA. The primers used for the amplification of the death and ligand binding domains of DR4 and DR5 TRAIL receptors are described in Table 1. DR4 and DR5 exon 9, coding for the death domain, was amplified in two overlapping fragments A and B including the intronic splicing sites and a portion of introns 8 and 9. Similarly, PCR fragments for exon 3 and 4 also included the splicing sites and adjacent intronic regions.

Amplifications were performed using a touchdown PCR (step-down PCR). Conditions were: 95°C for 5 min, three cycles with denaturation at 95°C for 30 s, annealing at 63°C for 30 s and extension at 72°C for 1 min, three cycles with annealing at 61°C, three cycles with annealing at 59°C, and 25 cycles with annealing at 58°C. The PCR products were electrophoresed on a 2% agarose gel stained with ethidium bromide, and band sizes were determined. All the amplifications were carried out in a Peltier PTC-225 Thermal Cycler (MJ Research).

WAVE detection system for DNA sequence changes

All amplified products were screened for the presence of sequence changes using the WAVE system (Transgenomic, Omaha, NE, USA). This system consists of ion-paired, denaturing high performance liquid chromatography (DHPLC) that analyzes the formation of heteroduplexes using different melting temperatures. The two sequences to be compared (wild type controls and tumor samples) are denatured and reannealed prior to DHPLC analysis to allow the formation of the original homoduplexes and possible mismatched heteroduplexes due to the presence of variations in the sequence. These heteroduplexes are thermally less stable and show reduced retention on the chromatographic separation matrix generating distinctly different peak profiles. In order to identify all the potential heteroduplexes, the chromatography was performed at three different melting temperatures. The normal and tumoral PCR products were mixed (2:3 ratio) and denatured at 94°C for 5 min followed by a 30-min ramp to 24°C (0.1°C/s). The denatured and reannealed samples were run on the WAVE instrument at different melting temperatures depending on the PCR products being analyzed. The gradient

V. Fernández et al.

Table 1. Primers for PCR and sequencing.

Identification letter	Fragment	Primer (Tm°C)	Length
TRAIL receptor DR4			
A	DR4-exon9-A F	5'-CCCAACTCATCTGGCTGTCT-3' (54.3)	273 bp
B	DR4-exon9-A R	5'-TGCATGTCTCTTCCATCC-3' (52.9)	
C	DR4-exon 9-B F	5'-ATGAAATGGGTCAACAAAACCTG-3' (52.4)	
D	DR4-exon 9-B R	5'-ACACCTAAGAGGAAACCTCTGG-3' (52.3)	
E	DR4-exon 3 F	5'-TTGGCTTTTCTCTCCCTTCC-3' (54.3)	206 bp
F	DR4-exon 3 R	5'-GCCCTCACTCCACCTCT-3' (54.4)	
G	DR4-exon 4 F	5'-AGGTC AAGGGACACGTCAGG-3' (58.5)	
H	DR4-exon 4 R	5'-GCTTCTGTGGTTTCTTGAGG-3' (52.7)	
TRAIL receptor DR5			
I	DR5-exon 9-A F	5'-CCAACCTCACCTGGCTGTCTC-3' (54.9)	263 bp
J	DR5-exon 9-A R	5'-AGCGTCTCCAAGGCATCC-3' (55.4)	
K	DR5-exon 9-B F	5'-CAGGATGCTGATAAAGTGGG-3' (53)	
L	DR5-exon 9-B R	5'-GGTCTGACTTCTGAAGAGA-3' (58.5)	
M	DR5-exon 3 F	5'-TTCTGGGAATCCTGTGGCAT-3' (56.6)	202 bp
N	DR5-exon 3 R	5'-CCCCGATTCCACCTTTA-3' (55.7)	
O	DR5-exon 4 F	5'-TTCCAAAACCTTATGCTCTG-3' (52.8)	
P	DR5-exon 4 R	5'-GGGGTCCATGGAGCTACTG-3' (55.6)	
Generation of positive controls			
Q	DR4-exon 9-mut-F	5'-CAGCATTGCTTACAAGGCAT-3' (52.7)	208 bp
R	DR4-exon 9-cut-R	5'-ACCCAGCTCTGATGCTGTTCC-3' (54.4)	
S	DR5-exon 9-mut-F	5'-CCTCAGCATTAGCCACCTTT-3' (53)	
T	DR5-exon 9-cut-R	5'-CAGTGCTTCGATGACTTTGC-3' (53.6)	
Effect at expression level of mutants of TRAIL receptor DR4			
U	DR4-exon3+4 F	5'-GGAGCCTGTAACCGGTGCAC-3' (58.9)	208 bp
V	DR4-exon3+4 R	5'-CTTCCGGCACATCTCAGCAG-3' (58.2)	
W	DR4-exon3+intron3 F	5'-CAGCTTGAAATCAGCCTGGAGT-3' (52.9)	
X	DR4-exon3+intron3 R	5'-CCCTCTGGAGCTGATAGTTTG-3' (53.8)	

for each PCR product was calculated using WAVEMaker software.

Generation of mutant positive controls

In order to have a positive control of nucleotide changes to use in the screening for gene mutations by the WAVE system we generated mutants for exon 9 of DR4 and DR5 by PCR technology (Figure 1). We adapted a previously described protocol for the introduction of point mutations in the middle region of a target.²² Briefly, exon 9 of DR4 and DR5 was amplified in two partially overlapping fragments. The longer fragment (fragment B) covered most of the sequence except a small 5' region. The shorter fragment (fragment A) covered the 5' sequence, including the sequence missing from fragment B, and carried a single nucleotide substitution introduced by primer design. DR4 fragment A was amplified with primers Q, carrying the mutation, and A (Table 1). DR4 fragment B was amplified with primers R and B. The primers used to amplify DR5 fragment A were S, carrying the mutation, and I whereas the primers for DR5 fragment B were T and J (Table 1).

Amplifications were performed using the touchdown PCR (step-down PCR) described above. PCR products were electrophoresed on a 2% agarose gel stained with ethidium bromide and purified using a GenElute PCR Clean-Up Kit (Sigma). The purified A and B fragments were mixed 1:1 and amplified with a touchdown PCR to generate a full exon 9 fragment that would contain a point mutation in the middle region. First, the PCR mix, containing fragments A and B but no primers, was subjected to an extension step consisting of 95°C for 5 min, 94°C for 30 s, 50°C for 30 s, and 72°C for 5 min. The primers A and B for the DR4 A mutant and I and J for the DR5 A mutant were added afterwards and then the PCR was performed. The mutants were electrophoresed, purified, and sequenced to confirm the nucleotide changes introduced.

DNA sequencing

PCR products showing abnormal chromatogram profiles in the WAVE analysis were sequenced. The amplified products were purified using a GenElute PCR Clean-Up Kit (Sigma) and sequenced using cycle sequencing

DR4 and DR5 in mantle cell lymphoma

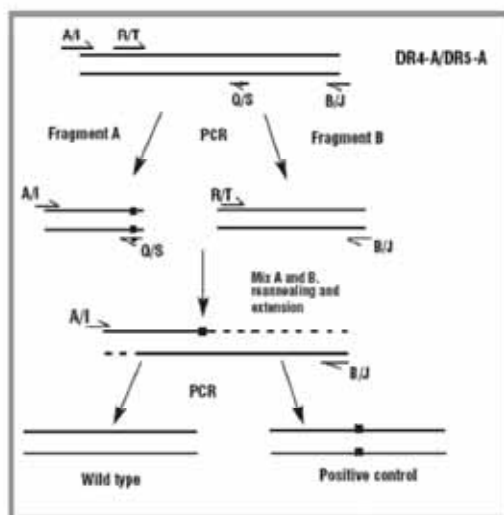


Figure 1. Generation of WAVE mutant positive controls. DR4 and DR5 exon 9 were amplified in two partially overlapping fragments: fragment A, which was the shorter of the two and carried the mutation (by amplification with mutated primer Q in DR4 or S in DR5, Table 1), and fragment B. Purified A and B PCR products were mixed 1:1 and subjected to a reannealing and extension step prior to amplification. The PCR products generated contained a point mutation in the middle region of exon 9.

with BigDye Terminator chemistry (Applied Biosystems, Foster City, CA, USA). Sequencing reactions were run on an Abi Prism ABI-3100 automated sequencer. All nucleotide changes were confirmed by sequencing both strands.

RNA extraction and reverse transcription PCR

Total RNA was obtained from frozen tissues using guanidine isothiocyanate extraction and cesium chloride gradient centrifugation. For cDNA synthesis, 1 µg of RNA and Taqman Reverse Transcriptions reagents (including Multiscribe™ reverse transcriptase and random hexamers) were used, as described by the manufacturer (Applied Biosystems). To examine the presence of the nucleotide change G1405T (Stop469Leu) of DR4 exon 9 in a sample for which only RNA was available, the coding region was amplified using primers C and D as described above. The potential effect at the RNA level of the two nucleotide changes detected in the TRAIL-R1/DR4 exon 3-intron 3 splicing region was studied by amplifying exon 3 and exon 4 coding regions near the exon-intron boundaries with primers U (exon 3) and V (exon 4); and exon 3-intron 3 with the primers W (including the splicing site nucleotide change) and X (intron 3).

Immunohistochemistry

DR4 protein expression was examined immunohistochemically on formalin-fixed, paraffin-embedded tissues using a murine monoclonal antibody (HS101) (Alexis Biochemicals, UK), standard antigen retrieval protocols, the Envision detection system (Dakocytomation, Carpinteria, CA, USA) and the automated immunostainer TechMate 500 Plus (Dako).

Statistical analyses

Differences in allele and genotype frequencies were determined among controls using the χ^2 test. Allele frequencies in the control group were evaluated for the Hardy-Weinberg equilibrium. The *p* value among controls for the A1322G polymorphism was 0.6, for the C626G it was 0.5 and for the G422A was 0.6. To test the hypothesis of an association between the different polymorphisms and lymphoid malignancies, multivariate methods were used based on logistic regression analysis. Cases were divided into groups and polytomous logistic regression was used comparing each group of cases with the whole set of controls. Odds ratios (OR) and 95% confidence intervals were calculated for each age (in tertiles) and sex adjusted group. Homozygosity for the more frequent allele among controls was set as the reference class for polymorphisms. The linear trend of the OR was tested using the categorized variable as quantitative after assigning a linear score to each ordered category.

Results

DR4 death domain

TRAIL receptor DR4 death domain is necessary for the transduction of the apoptotic signal and is encoded by exon 9. The majority of the DR4 mutations described in human tumors, including several types of lymphomas, have been detected in this region.^{7,17-21} The analysis of the 69 cases of MCL showed an anomalous pattern of DNA mobility in 24 (34.8%) of them (Figure 2). All cases showed an identical mobility profile, suggesting that it could correspond to a polymorphic variant. Sequencing analysis revealed that this anomalous pattern was due to the known polymorphism, A1322G, resulting in the conversion of the lysine at codon 441 to arginine. Only one of these 24 cases was homozygous for this variant. This polymorphism has been previously described in several cancer cell lines, human tumors, and in 2 of 10 (20%) healthy volunteers. This change seems to make the DR4 receptor less sensitive to the TRAIL signal.² To examine whether this polymorphism was more frequent in patients with MCL than in the healthy population we examined 91 DNA samples from normal controls. The A1322G polymorphism was signif-

V. Fernández et al.

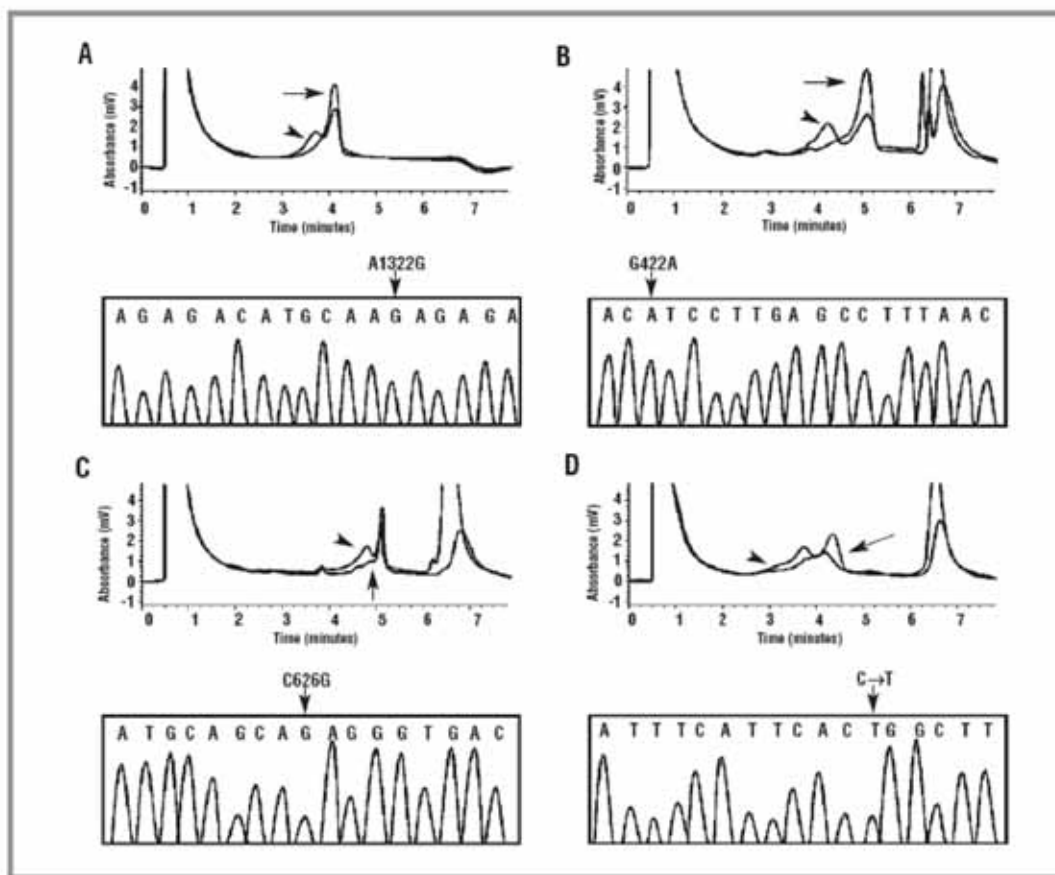


Figure 2. Polymorphisms in TRAIL receptors DR4 and DR5. Panels A, B, C and D represent the chromatogram (upper panel) and sequence (lower panel) of different DR4 and DR5 polymorphisms: (A) A1322G in the death domain of DR4; (B) G422A in the extracellular domain of DR4; (C) C626G in the extracellular domain of DR4; (D) Intronic polymorphism C→T at -21 Intron 3 of DR5. Arrow: normal, arrowhead: polymorphism.

icantly more common among patients with MCL, being present in 24 of 69 tumor samples (34.8%), as compared to in 16 of the 91 (17.6%) control samples. In MCL, the age- and sex-adjusted odds ratio (OR) for the presence of the G allele was 5.9 (95%CI=1.92-18.1); 5.2 (95% CI=1.64-16.1) in heterozygosity and 24.7 (95% CI=1.04-587.6) for the homozygous variant of the altered allele (Table 2).

To determine the possible presence of DR4 death domain mutations and the incidence of the A1322G polymorphism in other lymphoid neoplasms, the whole DR4 exon 9 was screened in 16 CLL, three of them with 8p deletions, 12 FL, 17 DLBCL and the four human lymphoid cell lines carrying the t(11;14) translocation. No mutations were detected in any of these cases. However, the A1322G polymorphism was observed in 6 (37.5%) CLL cases, which was a significantly higher

incidence than that in the controls (OR=4.5, 95% CI = 1.18-17). The polymorphism was identified in only in 1 (8.3%) FL and 3 (17.6%) DLBCL with an incidence similar to that in the normal population (Table 2). None of the cell lines analyzed had the polymorphic variant. Two samples from normal controls showed an abnormal pattern in their WAVE chromatograms, different from the characteristic A1322G profile (Figure 3). Cycle sequencing revealed a heterozygous alteration at nucleotide 1405 changing a guanine to thymine (G1405T) which leads to a substitution of the normal 469 stop codon for a leucine. This modification would encode for a putative DR4 protein variant with 14 additional amino acids. Intriguingly, one of these two normal individuals had a sister with acute myeloid leukemia who also shared this alteration in heterozygosity. This change was not detected in any of the 114 lymphoid tumors.

DR4 and DR5 in mantle cell lymphoma

Table 2. Allele frequency of A1322G in non-Hodgkin's lymphomas and odds ratio in relation to frequencies in controls.

Cases	Polymorphism	No. of cases	%	O.R. ¹	95% CI	Trend test	p value ²
Control population		91					
	A/A	75	82.4				
	A/G	15	16.5				
	G/G	1	1.1				
	A/G + G/G	16	17.6				
MCL		69				10.6	0.0011
	A/A	45	65.2	1	-		
	A/G	23	33.3	5.2	(1.64-16.1)		
	G/G	1	1.5	24.7	(1.04-587.6)		
	A/G + G/G	24	34.8	5.9	(1.92-18.1)		
CLL		16				5.9	0.0148
	A/A	10	62.5	1			
	A/G	5	31.	3.7	(0.92-14.9)		
	G/G	1	6.3	22.6	(1.03-495.9)		
	A/G + G/G	6	37.5	4.5	(1.18- 17)		
FL		12				0.2	0.6985
	A/A	11	91.7	1			
	A/G	1	8.3	0.7	(0.07-6.2)		
	G/G	0	0	0			
	A/G + G/G	1	8.3	0.7	(0.07-6.7)		
DLBCL		17				0.03	0.8625
	A/A	14	82.3	1			
	A/G	3	17.6	1.3	(0.29-5.6)		
	G/G	0	0	0			
	A/G + G/G	3	17.6	1.3	(0.29-5.5)		

¹OR: odds ratio; OR are adjusted for sex and age in tertiles; ²p-value for test of linear trend.

DR4 ligand-binding domain

A mutational analysis of exons 3 and 4 of TRAIL receptor DR4 was performed in the same series of MCL and other lymphoid neoplasms described above. These exons codify for the principal elements of the extracellular cysteine-rich domain of the receptor required for TRAIL binding. Sequence alterations in this region may lead to deficient ligand binding and affect the downstream apoptotic signaling.²³

Screening the genomic DNA revealed an abnormal chromatogram of the exon 3 fragment in two cases of typical MCL and one case of CLL. Sequencing analysis of these cases demonstrated three different nucleotide changes in the tumors (Figure 3). One MCL had a change in the splice site conserved sequence AGGT at the exon 3-intron 3 boundary, changing a guanine to cytosine at position +1 of intron 3. The second MCL had a change near the splicing site at position +6 of intron 3, also changing a guanine to cytosine. The CLL showed a silent change at nucleotide 465 changing an adenine for a cytosine (Thr155Thr). All three cases were heterozygous for the altered allele. These changes were also detected in the germ-line of the patients but in none of the 91 healthy controls. To analyze the potential effect of these changes at the RNA level, cDNA from the two

cases of MCL was generated and amplified with two different sets of primers. The first set consisted in primers which amplified exon 3 and exon 4 coding regions near the exon-intron boundaries and the second set consisted in a forward primer that carried the mutation corresponding to each case, and a reverse primer which annealed to a near region in intron 3 (Table 1). Genomic DNA from the cases was used as the positive control. No anomalous transcripts were detected in these lymphomas suggesting that these changes may not be functionally relevant.

In addition to these distinct chromatograms, two anomalous profiles were detected in more than one case suggesting that they could correspond to polymorphic variants (Figure 2). Sequencing analysis revealed two previously described polymorphisms: G422A and C626G at exon 3 and 4, respectively.²³ These changes result in a substitution of a histidine for arginine and an arginine for threonine, respectively. These two polymorphic variants seem to co-segregate homozygously in patients with lung, head and neck, and gastric cancer, in whom their incidence is significantly higher than in healthy controls.²³ To determine whether these polymorphisms were differentially represented in patients with lymphoid neoplasms we also screened a series of 91 healthy

V. Fernández et al.

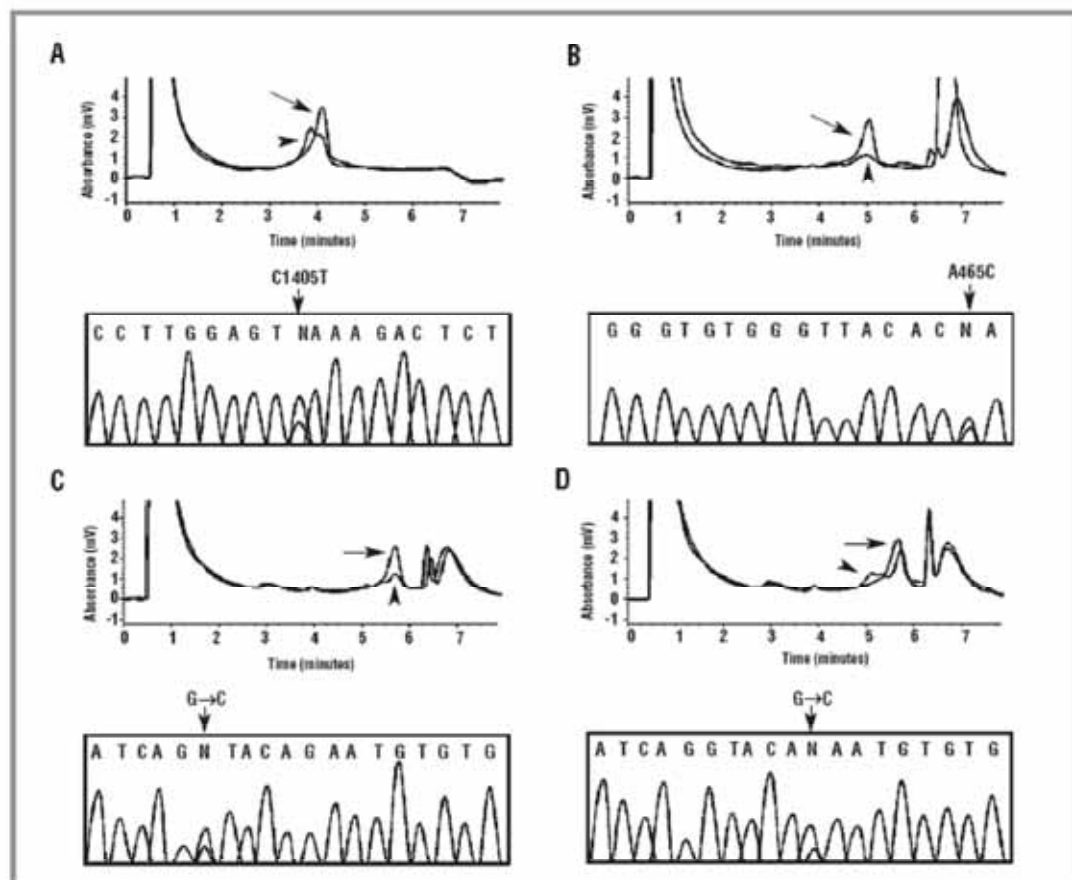


Figure 3. Nucleotide changes in TRAIL receptor DR4. Panels A, B, C and D represent the chromatograms (upper panels) and sequences (lower panels) of different nucleotide changes: (A) G1405T in the death domain; (B) silent mutation A465C at exon 3, in the extracellular domain; (C) G→C at position +1 of the splicing donor site of intron 3; (D) G→C at position +6 of the splicing donor site of intron 3. Arrow: normal, arrowhead: nucleotide change.

controls. The distribution of the CC, CG, and GG alleles of exon 4 C626G polymorphism in the different lymphoma types is shown in Table 3. The frequency of the alleles was similar in CLL, FL, DLBCL and the control population after adjustment for age and sex. However, the presence of the G allele was associated with an overall significant protective effect in MCL compared to in the controls (OR=0.3, 95%CI=0.12-0.8). The G422A variant was also observed at the same allelic frequency in all types of lymphoid tumors and controls (data not shown). Interestingly, a significant association between the homozygous A allele of this polymorphism and the homozygous G allele of codon 626 was observed in MCL since 7 of the 14 MCL patients (50%) homozygous for the 422 AA allele were also homozygous for the 626 GG allele whereas this association was only detected in 3 of the 27 (11%) controls homozygous for the G422A polymorphism ($p=0.04$).

To determine whether these polymorphic variants were associated with different DR4 protein expression we examined 12 cases of MCL by immunohistochemistry: 6 had the A1322G variant, 8 the C626G variant and 9 the G422A variant. The intensity of DR4 expression was similar in all cases, indicating that DR4 is expressed in all MCL independently of the polymorphic variant.

DR5 death and ligand-binding domains

The TRAIL receptor DR5 death and ligand-binding domains were similarly examined in the 114 lymphoid neoplasms and 91 healthy controls. No mutations or polymorphic variants were detected in the coding regions or splicing sites of exons 3, 4 or 9, of any of the tumors or controls analyzed. Only a common nucleotide change (T for a C) in intron 2, at position -21 from the start of exon 3, was observed in most of the cases studied. The

DR4 and DR5 in mantle cell lymphoma

Table 3. Allele frequency of C626G in non-Hodgkin's lymphomas and odds ratio in relation to frequencies in controls.

Cases	Polymorphism	No. of cases	%	O.R. ¹	95% CI	Trend test	p value ²
Control population	91						
	C/C	26	28.6				
	C/G	49	53.9				
	G/G	16	17.6				
	C/G + G/G	65	71.4				
MCL		69				3.5	0.0633
	C/C	34	49.3	1	-		
	C/G	17	24.6	0.4	(0.12-1.1)		
	G/G	18	26.1	0.4	(0.12-1.1)		
	C/G + G/G	35	50.7	0.3	(0.12-0.8)		
CLL		12				2.4	0.1198
	C/C	2	16.7	1	-		
	C/G	2	16.7	0.6	(0.08-4.9)		
	G/G	8	66.7	3.6	(0.62-20.8)		
	C/G + G/G	10	83.3	1.6	(0.31-8.6)		
FL		12				0.5	0.4884
	C/C	5	41.7	1	-		
	C/G	3	25.0	0.5	(0.09-2.5)		
	G/G	4	33.3	0.6	(0.12-2.8)		
	C/G + G/G	7	58.3	0.5	(0.12-1.8)		
DLBCL		17				2.1	0.1454
	C/C	5	29.4	1	-		
	C/G	1	5.9	0	-		
	G/G	11	64.7	2.4	(0.66-9.0)		
	C/G + G/G	12	70.6	0.8	(0.24-2.7)		

¹OR: odds ratio; OR are adjusted for sex and age in tertiles; ²p-value for test of linear trend.

frequencies ranged from 77% to 100% in different lymphoma groups, and 86% in normal controls indicating that this must be the most common DR5 sequence in the control population (Figure 2). No significant differences were observed between the different lymphoid tumors and the healthy population.

Discussion

DR4 and DR5 TRAIL receptors have been mapped to chromosome 8p21-22 bands.^{10,20} This genetic region is frequently deleted in different human tumors suggesting that it may harbor a potential tumor suppressor gene. Inactivating mutations of DR4 and DR5 receptors have been associated with loss of heterozygosity in some tumors, indicating that these genes may be potential targets of 8p deletions.^{10,20} DR4 and DR5 mutations have been observed in head and neck squamous cell carcinomas, non-small cell lung carcinomas, breast and gastric cancers, and non-Hodgkin's lymphomas. Most of these mutations were detected in the death domain and intronic sequences of the genes and consisted of missense alterations and less frequently non-sense, microdeletions, splice-site, and silent mutations.^{1,17-22,24,26}

In our study, we detected three nucleotide changes in the DR4 extracellular domain of two patients with MCL and one with CLL. These changes involved position +1 of the intron 3 splice-site donor consensus sequence and position +6 of the same intron in the two cases of MCL respectively, and a silent mutation in codon 155 in the CLL. These three changes were in heterozygosis and were not detected in any of the control samples examined. However, they were also present in the germ-line of the patients and the changes in the splicing sites were not associated with anomalous transcripts, suggesting that they may be rare polymorphisms with no apparent functional significance. Deletions of chromosome 8p were found in 6 tumors (3 CLL and 3 MCL) but none of these cases had mutations in the DR4 extracellular domain. This lack of inactivating mutations in our study is in contrast with the only previous report on non-Hodgkin's lymphomas in a Korean population in which 7% of the tumors showed potential inactivating mutations in the death domain of DR4 or DR5 genes.¹⁷ This difference may be due in part to the spectrum of tumors examined since the previous study included only 3 MCL, 7 CLL, and 4 FL whereas mutations were detected in 5 of 46 (11%) DLBCL, 2 of 23 (9%) MALT lymphomas and 1 of 14 (7%) peripheral T-cell lymphomas. However, a similar differ-

V. Fernández et al.

ence in the incidence of TRAIL receptor mutations in Korean and Western populations has been observed in solid tumors. Thus, DR4 or DR5 mutations were noted in 11% of non-small cell lung cancers (NSCLC) and 30% of metastatic breast carcinomas in the Korean population, but in only 3% of head and neck carcinomas, and in none of a large series of NSCLC and breast tumors in Western patients, suggesting a possible population-based difference in the mutation pattern of these genes.^{18-21,24}

Although DR4 and DR5 inactivating mutations were not detected in our series, two polymorphic changes in the DR4 death and ligand binding domains were more frequently detected in different types of lymphoid neoplasms than in the normal control population. The DR4 death domain A1322G polymorphism was present in 37.5% and 34.8% of CLL and MCL patients, respectively, but in only 17.6% of the control population. These differences were statistically significant when compared to a sex- and age-adjusted healthy population, suggesting that this polymorphism may be associated with an increased risk of developing these tumors. The allelic frequencies in FL and DLBCL were similar to those in the normal controls. Transfection experiments in ovarian and bladder cancer cell lines have shown that this polymorphism has a dominant negative effect in DR4-mediated killing, rendering cells more resistant to TRAIL.⁴ Although this polymorphism may not alone justify complete resistance to TRAIL, its dominant negative effect *in vitro* may explain its heterozygous predominance and suggest a certain contribution to apoptotic resistance facilitating the development of CLL and MCL neoplastic clones.^{6,19}

Two additional polymorphisms in the DR4 ligand-binding domain, G422A and C626G, have been associated in homozygosity with an increased risk of different solid tumors. Thus, G422A was found to be associated with gastric, lung, and head and neck cancers whereas C626G was found to be overrepresented in lung, and head and neck tumors.²⁵ In contrast, the C626G polymorphism had a protective effect in patients with bladder cancer. The DR4 extracellular domain was not examined in the previous study of NHL and, therefore, no information on the distribution of these polymorphisms in lymphoid neoplasms is available.¹⁹ In our study, the frequency of the G422A allele was similar in all types of lymphomas and healthy controls. However, the C626G variant was associated with a significant protective effect for MCL. In urinary bladder carcinomas, the protective effect of this polymorphism was mainly associated with young, light smokers suggesting an association between the development of the tumor, the DR4 polymorphism, and environmental exposure.²⁵ Epidemiological risk factors in MCL have not been studied and, therefore, the possible rela-

tionship of this association and an environmental exposure in such patients is not known. The GG and AA homozygous variants of the 626 and 422 polymorphisms co-segregated in 44-48% of patients with head and neck, lung and gastric carcinomas.²⁵ Interestingly, the frequency of being homozygous for both alleles was also significantly higher in MCL patients than in controls, suggesting that this association may be common in different types of tumors. The functional effect of these polymorphisms is currently unknown. However, their location flanking the receptor ligand interface regions suggest that sequence changes may alter binding of the ligand to the receptor and apoptotic signaling.

Since TRAIL has a selective action, being more apoptotic to tumor cells than to normal cells, it has been suggested that it could be used as a new therapeutic strategy.^{13,26} However, the sensitivity of different tumors to TRAIL-induced apoptosis is variable and the determinants of the different responses are not well known. Primary CLL cells and other hematologic malignancies may be resistant to the TRAIL effect.^{13,40} The causes of this resistance appear to be complex, involving different factors such as variable levels of expression of the receptor and other elements of the downstream pathway.¹³ The rare presence of inactivating mutations in DR4 and DR5 genes in our series of lymphoid neoplasms, including 6 cases with 8p deletions, indicate that these alterations are not relevant cause of TRAIL resistance. However, the relatively high frequency of several DR4 polymorphisms with a potential functional effect in MCL and CLL suggests that polymorphic variants may play a role in TRAIL resistance in such neoplasms. In addition, the significantly different frequencies of these polymorphic variants in tumors compared with in the normal population suggests that they may also act as genetic modulators in the development of certain malignancies.

VF and PJ examined the presence of mutations and polymorphisms in all cases and healthy controls. SB and JS analyzed the chromosomal alterations of these tumors by comparative genomic hybridization. EG and SS performed the statistical analysis. DC and EM selected all the patients with CLL, some of those with MCL, and the healthy controls. GO and EC reviewed all the pathology samples of the lymphomas. VF and PJ drafted the manuscript and EC wrote the final version. EC, PJ and DC designed the whole study. All authors critically reviewed the final version of the manuscript. We thank Iracema Nayach, Montse Sanchez and Laura Pla for their excellent technical assistance, and David Escuderos for his skilful help in the making of the figures.

The authors reported no potential conflicts of interest.

Supported by Grants SAF2002/03261 from Comisión Interministerial de Ciencia y Tecnología, Red de Genómica de Cáncer 03/10 y de Estudio de Neoplasias Linfoides 03/179, Instituto Nacional de Salud Carlos III-Ministry of Health, Generalitat de Catalunya 2000SGR00118 and FIS 03103.

Verónica Fernández is a recipient of a predoctoral fellowship from the Spanish Ministry of Science and Technology.

Manuscript received March 26, 2004. Accepted August 14, 2004.

References

- Baetu TM, Hiscott J. On the TRAIL to apoptosis. *Cytokine Growth Factor Rev* 2002;13:199-207.
- Daniel PT, Wiedler T, Sturm I, Schulze-Osthoff K. The kiss of death: promises and failures of death receptors and ligands in cancer therapy. *Leukemia* 2001;15:1022-32.
- Sheikh MS, Fornace AJ Jr. Death and decoy receptors and p53-mediated apoptosis. *Leukemia* 2000;14:1509-13.
- Fesik SW. Insights into programmed cell death through structural biology. *Cell* 2000;103:273-82.
- Degli-Esposti M. To die or not to die—the quest of the TRAIL receptors. *J Leukoc Biol* 1999;65:535-42.
- Kim K, Fisher MJ, Xu SQ, El Deiry WS. Molecular determinants of response to TRAIL in killing of normal and cancer cells. *Clin Cancer Res* 2000;6:335-46.
- Arai T, Akiyama Y, Okabe S, Saito K, Iwai T, Yuasa Y. Genomic organization and mutation analyses of the DR5/TRAIL receptor 2 gene in colorectal carcinomas. *Cancer Lett* 1998;133:197-204.
- Pan G, O'Rourke K, Chinnaiyan AM, Gentz R, Ebner R, Ni J, et al. The receptor for the cytotoxic ligand TRAIL. *Science* 1997;276:111-3.
- Sheridan JP, Marsters SA, Pitti RM, Gurney A, Skubatch M, Baldwin D, et al. Control of TRAIL-induced apoptosis by a family of signaling and decoy receptors. *Science* 1997;277:818-21.
- MacFarlane M, Ahmad M, Srinivasula SM, Fernandes-Alnemri I, Cohen GM, Alnemri ES. Identification and molecular cloning of two novel receptors for the cytotoxic ligand TRAIL. *J Biol Chem* 1997;272:25417-20.
- Walczak H, Degli-Esposti MA, Johnson RS, Smolak PJ, Waugh JY, Boiani N, et al. TRAIL-R2: a novel apoptosis-mediating receptor for TRAIL. *EMBO J* 1997;16:5386-97.
- Hymowitz SG, Christinger HW, Fuh G, Ullsch M, O'Connell M, Kelley RF, et al. Triggering cell death: the crystal structure of Apo2L/TRAIL in a complex with death receptor 5. *Mol Cell* 1999;4:563-71.
- MacFarlane M, Harper N, Snowden RT, Dyer MJ, Barnett GA, Pringle JH, et al. Mechanisms of resistance to TRAIL-induced apoptosis in primary B cell chronic lymphocytic leukaemia. *Oncogene* 2002;21:6809-18.
- Rieck-Laucat F, Le Deist F, Hivroz C, Roberts IA, Debatin KM, Fischer A, et al. Mutations in Fas associated with human lymphoproliferative syndrome and autoimmunity. *Science* 1995;268:1347-9.
- Straus SE, Jaffe ES, Puck JM, Dale JK, Elkon KB, Rosen-Wolff A, et al. The development of lymphomas in families with autoimmune lymphoproliferative syndrome with germline Fas mutations and defective lymphocyte apoptosis. *Blood* 2001;98:194-0.
- Gronbaek K, Straten PT, Ralfkiaer E, Ahrenkiel V, Andersen MK, Hansen NE, et al. Somatic Fas mutations in non-Hodgkin's lymphoma: association with extranodal disease and autoimmunity. *Blood* 1998;92:3018-24.
- Lee SH, Shin MS, Kim HS, Lee HK, Park WS, Kim SY, et al. Somatic mutations of TRAIL-receptor 1 and TRAIL-receptor 2 genes in non-Hodgkin's lymphoma. *Oncogene* 2001;20:399-403.
- Shin MS, Kim HS, Lee SH, Park WS, Kim SY, Park JY, et al. Mutations of tumor necrosis factor-related apoptosis-inducing ligand receptor 1 (TRAIL-R1) and receptor 2 (TRAIL-R2) genes in metastatic breast cancers. *Cancer Res* 2001;61:4942-6.
- Seitz S, Wassmuth P, Fischer J, Nothnagel A, Jandrig B, Schlag PM, et al. Mutation analysis and mRNA expression of TRAIL-receptors in human breast cancer. *Int J Cancer* 2002;102:117-28.
- Lee SH, Shin MS, Kim HS, Lee HK, Park WS, Kim SY, et al. Alterations of the DR5/TRAIL receptor 2 gene in non-small cell lung cancers. *Cancer Res* 1999;59:5683-6.
- Pai SI, Wu GS, Ozoren N, Wu L, Jen J, Sidransky D, et al. Rare loss-of-function mutation of a death receptor gene in head and neck cancer. *Cancer Res* 1998;58:3513-8.
- Park WS, Lee JH, Shin MS, Park JY, Kim HS, Kim YS, et al. Inactivating mutations of KILLER/DR5 gene in gastric cancers. *Gastroenterology* 2001;121:1219-25.
- Fisher MJ, Virmani AK, Wu L, Aplenc R, Harper JC, Powell SM, et al. Nucleotide substitution in the ectodomain of TRAIL-receptor DR4 is associated with lung cancer and head and neck cancer. *Clin Cancer Res* 2001;7:1688-97.
- Sibley K, Rollinson S, Allan JM, Smith AG, Law GR, Roddam PL, et al. Functional FAS promoter polymorphisms are associated with increased risk of acute myeloid leukemia. *Cancer Res* 2003;63:4327-30.
- Lai HC, Sytwu HK, Sun CA, Yu MH, Yu CP, Liu HS, et al. Single nucleotide polymorphism at Fas promoter is associated with cervical carcinogenesis. *Int J Cancer* 2003;103:221-5.
- Campo E, Raffeld M, Jaffe ES. Mantle-cell lymphoma. *Semin Hematol* 1999;36:115-27.
- Degli-Esposti MA, Smolak PJ, Walczak H, Waugh J, Huang CP, DuBose RF, et al. Cloning and characterization of TRAIL-R3, a novel member of the emerging TRAIL receptor family. *J Exp Med* 1997;186:1165-70.
- Walczak H, Degli-Esposti MA, Johnson RS, Smolak PJ, Waugh JY, Boiani N, et al. TRAIL-R2: a novel apoptosis-mediating receptor for TRAIL. *EMBO J* 1997;16:5386-97.
- Martinez-Climent JA, Vizcarra E, Sanchez D, Blesa D, Marugan I, Benet I, et al. Loss of a novel tumor suppressor gene locus at chromosome 8p is associated with leukemic mantle cell lymphoma. *Blood* 2001;98:3479-82.
- Bea S, Ribas M, Hernandez JM, Bosch F, Pinyol M, Hernandez L, et al. Increased number of chromosomal imbalances and high-level DNA amplifications in mantle cell lymphoma are associated with blastoid variants. *Blood* 1999;93:4365-74.
- Bea S, Lopez-Guillermo A, Ribas M, Puig X, Pinyol M, Carrio A, et al. Genetic imbalances in progressed B-cell chronic lymphocytic leukemia and transformed large-cell lymphoma (Richter's syndrome). *Am J Pathol* 2002;161:957-68.
- Meeteel AR, Rao MR. Generation of multiple site-specific mutations by polymerase chain reaction. *Methods Mol Biol* 2002;182:95-102.
- Marsters SA, Sheridan JP, Pitti RM, Huang A, Skubatch M, Baldwin D, et al. A novel receptor for Apo2L/TRAIL contains a truncated death domain. *Curr Biol* 1997;7:1003-6.
- Ozoren N, El Deiry WS. Cell surface Death Receptor signaling in normal and cancer cells. *Semin Cancer Biol* 2003;13:135-47.
- McDonald ER III, Chui PC, Martelli PF, Dicker DT, El Deiry WS. Death domain mutagenesis of KILLER/DR5 reveals residues critical for apoptotic signaling. *J Biol Chem* 2001;276:14939-45.
- Wu WG, Soria JC, Wang L, Kemp BL, Mao L. TRAIL-R2 is not correlated with p53 status and is rarely mutated in non-small cell lung cancer. *Anticancer Res* 2000;20:4525-9.
- Hazra A, Chamberlain RM, Grossman HB, Zhu Y, Spitz MR, Wu X. Death receptor 4 and bladder cancer risk. *Cancer Res* 2003;63:1157-9.
- Ashkenazi A, Pai RC, Fong S, Leung S, Lawrence DA, Marsters SA, et al. Safety and antitumor activity of recombinant soluble Apo2 ligand. *J Clin Invest* 1999;104:155-62.
- Walczak H, Miller RE, Ariail K, Gliniak B, Griffith TS, Kubin M, et al. Tumoricidal activity of tumor necrosis factor-related apoptosis-inducing ligand in vivo. *Nat Med* 1999;5:157-63.
- Snell V, Clodi K, Zhao S, Goodwin R, Thomas EK, Morris SW, et al. Activity of TNF-related apoptosis-inducing ligand (TRAIL) in hematological malignancies. *Br J Haematol* 1997;99:618-24.

DR4 and DR5 in mantle cell lymphoma

TREBALL 3: LA PROGRESSIÓ EN LEUCÈMIA LIMFÀTICA CRÒNICA

**Evolució del perfil genòmic i d'expressió en la progressió clínica
primerenca de la leucèmia limfàtica crònica**

Haematologica 2007 (Acceptat)

(Journal impact factor 2006: 5.032)

Evolució del perfil genòmic i d'expressió en la progressió clínica primerenca de la leucèmia limfàtica crònica

Els mecanismes biològics implicats en la progressió clínica primerenca dels pacients amb leucèmia limfàtica crònica (CLL) no es coneixen del tot bé. Hem estudiat mostres seqüencials de 16 pacients de CLL no tractats, obtingudes al diagnòstic i després de la progressió clínica i abans del tractament. Un pacient presentava una deleció homozigota del gen p16^{INK4a} en ambdues mostres, i tres pacients van adquirir una mutació del gen p53, guanys de les regions cromosòmiques 5q21-q23 i 11pter-p14, i un guany del cromosoma 12, respectivament, durant la progressió de la malaltia. L'anàlisi de l'expressió gènica va mostrar una modulació significativa de 58 gens, especialment la disminució de l'expressió de gens que actuen com inhibidors de l'adhesió i motilitat cel·lulars.

* La contribució personal en aquest treball ha estat la participació en el disseny experimental del projecte, l'extracció de material genètic de les mostres (DNA i RNA) i posterior caracterització molecular dels tumors (estat mutacional dels gens de la cadena pesada de les immunoglobulines, p53 i p16^{INK4a}), l'estudi de l'expressió gènica dels casos mitjançant la tecnologia dels microarrays, així com la interpretació dels resultats, l'anàlisi de dades, i la redacció del treball.

GENE EXPRESSION PROFILE AND GENOMIC CHANGES IN DISEASE PROGRESSION OF EARLY-STAGE CHRONIC LYMPHOCYTIC LEUKEMIA

Verònica Fernández¹, Pedro Jares², Itziar Salaverria¹, Eva Giné³, Sílvia Beà¹, Marta Aymerich¹, Dolors Colomer¹, Neus Villamor¹, Francesc Bosch³, Emili Montserrat³, Elias Campo¹

¹Hematopathology Section, Department of Pathology, ²Genomics Unit, and ³Department of Hematology, Hospital Clínic, Institut d'Investigacions Biomèdiques August Pi i Sunyer (IDIBAPS), University of Barcelona, Barcelona, Spain.

Running Title: Genetic and Molecular evolution in CLL

Keywords: Chronic lymphocytic leukemia, progression, microarrays, comparative genomic hybridization

Word count: 1550

Acknowledgments: the authors would like to thank Montserrat Sánchez, Laura Pla, Dr. Patricia Pérez-Galán and Jordi Altirriba for his helpful collaboration in this project. Supported by Grants CICYT SAF 05/5855 from the Spanish Ministry of Science, FIS 05/0213 and ISCIII-RETIC RD06/0020 from Ministry of Health, and Generalitat de Catalunya 2005SGRO870. Verònica Fernández is a recipient of a predoctoral fellowship from Spanish Ministry of Education and Science (MEC).

Corresponding author: Elias Campo, Hematopathology Unit, Hospital Clínic, Villarroel 170, 08036-Barcelona, Spain. Phone 34 93-227 5450, fax 34 93 227 5572; e-mail: ecampo@clinic.ub.es

SUMMARY

The biological mechanisms involved in the clinical progression from early stages of patients with chronic lymphocytic leukemia (CLL) are not well known. We investigated sequential samples from 16 CLL untreated patients obtained at diagnosis in early stage and after progression before treatment. One patient had a p16^{INK4a} homozygous deletion at diagnosis and progression, and three patients acquired a p53 mutation, gains of 5q21-q23 and 11pter-p14, and a gain of chromosome 12, respectively, during the progression of the disease. Gene expression profile analysis showed a significant modulation of 58 genes with a particular downregulation of genes that are inhibitors of cell adhesion and motility.

INTRODUCTION

Chronic lymphocytic leukemia (CLL) is the most common leukemia in adults in Western countries and it is characterized by a clonal proliferation and accumulation of mature neoplastic CD5+ B lymphocytes. The individual clinical course of these patients is extremely variable¹. Patients with CLL in early stage may not require treatment for several years but half of them will progress to a more advanced stage and will need treatment. The median time to disease progression and therapeutic requirement is shorter in patients with unmutated immunoglobulin genes (U-CLL), increased ZAP-70 expression, or adverse cytogenetic alterations¹. Tumor progression into advanced stages and transformation into large B-cell lymphoma has been associated with diverse factors, such as karyotypic evolution², oncogenic alterations of cell cycle regulatory genes³ and inactivation of tumor suppressor genes^{4,5}. However, the mechanisms that may be involved in the progression of the disease in early stages before the patient requires treatment have not been examined.

To determine possible genetic and molecular alterations related to early clinical progression in CLL, we investigated the genomic and gene expression profile alterations in a series of sequential samples obtained at diagnosis in early stage and at the time of clinical progression before treatment.

MATERIAL AND METHODS

Patient's selection

Sixteen patients diagnosed with CLL were selected based on the availability of two sequential peripheral-blood cell samples in which the first was obtained at diagnosis in an early clinical stage (Binet stage A) and the second one when the patient had an active disease but before the onset of treatment (Binet stage B=10 cases and C=6 cases). Active disease was defined according to standard criteria as follows: evidence of progressive marrow failure, massive or progressive splenomegaly or lymphadenopathy, progressive lymphocytosis or lymphocyte doubling time inferior to 6 months, autoimmune phenomena poorly responsive to corticosteroid therapy, or presence of disease related symptoms^{6,7}. For comparison, sequential samples from three patients with stable CLL disease were also included in the study. All patients gave an informed consent according to the Institutional Ethic Committee. The clinical details of the patients are provided in Table 1.

Isolation of tumor cells, purification and ZAP-70 analysis

Mononuclear cells were isolated from peripheral blood by gradient centrifugation, frozen in DMSO and stored at -180°C until analysis. Samples were thawed and tumor cells were purified using anti-CD19 magnetic microbeads (Miltenyi Biotech[®], Bergisch Gladbach, Germany) prior to nucleic acid extraction. A purity greater than 98% of CLL cells was obtained in all samples. The expression of ZAP-70 was determined by flow cytometry as described⁸.

DNA analysis

DNA was isolated according to standard protocols. Comparative genomic hybridization (CGH), the mutational status of the immunoglobulin heavy chain genes (IgV_H), p53 mutations, and p16^{INK4a} deletions were performed as previously described in all sequential samples^{2,8,9}.

RNA extraction and microarray analysis

Total RNA was extracted with the TRIzol[®] reagent (Invitrogen Life Technologies[®], Carlsbad, CA, USA). High quality RNA samples were hybridized to HU133plus2.0 GeneChips (Affymetrix[®], Santa Clara, CA, USA), and processed according to standard protocols. Data normalization was performed with the GeneChip[®] Operating Software (GCOS, Affymetrix[®]) and using the global scaling method (target intensity=500). The data was then filtered with the DNA-Chip analyzer software v1.3 (dChip, Boston, MA, USA). To perform the unsupervised analysis, genes were filtered according to their variation across samples ($1 < \text{standard deviation for logged data} < 10$) and the expression level (≥ 5 in $\geq 30\%$ samples). For the supervised analysis, only the probe sets with values above 10 for at least the 60% of the samples were considered for further analysis. Differential expression of paired samples was assessed with the Linear Model for Microarray Data Analysis (LIMMA) software package¹⁰. The genes considered as significant were those which met both conditions of $p\text{-value} < 0.05$ (corrected using the False Discovery Rate method) and Bayes statistic $(B) > 1$. Clusters were built with the dChip software. Gene identity and functional annotation was studied with the Ingenuity Pathways Analysis[®] v.4.0 program (Redwood City, CA, USA).

Real time quantitative RT-PCR (qRT-PCR) validation

cDNA was synthesized from 1 mg of total RNA by using the High-Capacity cDNA Archive kit (Applied Biosystems[®]). *ACTL6A*, *OGG1*, *PLCB2* and *RAPGEF1* expression

levels were determined with the following pre-developed assays (Applied Biosystems[®]): *ACTL6A* Hs00188792_m1; *OGG1* Hs00213454_m1; *PLCB2* Hs00190117_m1 and *RAPGEF1* Hs00178409_m1. Expression levels were calculated with the $2^{-\Delta\Delta Ct}$ method using human β -glucuronidase (GUS) as endogenous control. The differences of expression between sequential samples were analysed using a paired-T test approach (BRB-Array Tools v.3.3.0 software[®], National Cancer Institute, USA).

RESULTS AND DISCUSSION

IgV_H and ZAP-70 status

All sequential samples were clonally related showing the same immunoglobulin heavy chain genes (IgV_H) family switch and mutational status (Table 1). Fifteen of the 16 cases with progressive disease were unmutated and the sequence was stable during the evolution of the disease. 12 of the 15 unmutated cases were ZAP-70 positive. Two of the three discordant unmutated CLL had a 17p deletion (*CLL8*) and a 11q loss (*CLL16*) respectively, a common finding in CLL with discordance between the IgV_H mutational status and ZAP-70 expression¹¹. The 3 patients with stable disease (*CLL control 1-3*) had CLL with unmutated for the IgV_H genes and ZAP-70 positive.

Comparative Genomic Hybridization (CGH)

The CGH profiles showed a global low number of chromosomal alterations in all the patients (Table 1, Figure 1). Chromosomal imbalances were detected in 9 of the 16 (56%) initial samples from CLL with clinical progression. The most common alteration was trisomy 12 (27 %). Two patients with a non-altered initial genomic profile acquired new karyotypic aberrations: a gain of 5q21-q23 and 11pter-p14 (*CLL3*) and a gain of chromosome 12 (*CLL9*), respectively. Gains of 5q and 11p are uncommon in CLL but have been observed in cases with complex karyotypes^{12;13}, although their association with disease progression had not been previously observed. Interestingly, the patient that acquired trisomy 12 as a single alteration upon disease progression subsequently developed transformation into a large B-cell lymphoma in 35 months. Clonal evolution in CLL has been documented in occasional studies, usually associated with advanced disease and shorter survival^{2;14}. Our observations indicate that a moderate increase of chromosomal imbalances may occur already in early phases of clinical progression in CLL.

P53 and p16 status

In the present series two patients had an inactivation of the two tumor suppressor genes p53 and p16^{INK4a} at tumor progression (Table 1). One case (*CLL8*) with a 17p loss at diagnosis acquired the p53 mutation during the progression of the disease, supporting the notion that inactivation of this tumor suppressor gene in CLL may occur early in disease progression ¹⁴. Concerning the p16^{INK4a} locus, one case (*CLL10*) had a homozygous deletion in both sequential samples, associated with a small deletion of 9pter-p23 observed by CGH. The case with a p53 mutation also had a loss of 9pter-p23, but in this case p16^{INK4a} was not deleted, confirming previous observations that 9p losses in CLL are not always associated with p16^{INK4a} gene aberrations ².

Microarrays data analysis

The unsupervised analysis of the 26 paired samples from 13 patients (*CLL1-CLL13*) failed to identify the two groups of samples at diagnosis and progression, indicating that the individual variations in the expression profile were higher than the differences related to the behavior of the disease. These observations are in line with the results obtained in a previous gene expression profile study that compared unrelated tumor samples from progressed and stable CLL and did not find single genes significantly associated with this phenomenon ¹⁵. However, the supervised analysis comparing the initial and progressed sample of the same patients allowed us to identify a group of 58 genes differentially expressed in these two situations (Figure 2A, Supplementary Table 1). 37 genes were overexpressed (fold-change ratio between 0.3 and 1.7) whereas 21 were downregulated (fold-change ratio between -0.3 and -2). No significant differences were observed in the expression of these genes in the sequential samples of the 3 CLL cases with stable clinical evolution (Figure 2B). The functional analysis of the upregulated genes showed that they are involved in different pathways (Supplementary Figure 2), including cell cycle and cell growth (*MCM4*, *RAPGEF2*, *OGG1*, *ESCO1*, *ESR1*, *ACTL6A*, *CENPJ*, *ATG5*) and calcium and ion regulation (*MYLC2PL*, *ADRB1*, *TRPV5*, *TMCO3*). Interestingly, 6 of the 21 (29%) downregulated genes are considered negative regulators of integrin mediated cell adhesion and motility (*PRAM1*, *CDC42EP4*, *COL4A2*, *PLCB2*, *RAPGEF1*, *FLNA*). These findings are concordant with recent experimental studies suggesting that CLL progression is associated with increased ability to respond to migratory signals and that ZAP-70 positive tumors are more sensitive to these signals ^{16;17}.

Four genes were further chosen to validate the microarray results by qRT-PCR; according to their higher variation between samples, B-statistic score and biological meaning. These four genes were *ACTL6A* (upregulated, cell cycle and cell growth pathway), *OGG1* (upregulated, cell cycle and cell growth pathway), *RAPGEF1* (downregulated, cell adhesion and motility pathway) and *PLCB2* (downregulated, cell adhesion and motility pathway). The validation was performed in 10 paired samples from the microarray study and 3 new paired samples (*CLL14-CLL16*) (Table 1, Supplementary Figure 1). The microarray results were confirmed in all cases.

In summary, our results indicate that clinical progression of early stage CLL is associated with karyotype evolution, inactivation of tumor suppressor genes and modulation of the expression of a small number of genes, specially a subset that are inhibitors of cell adhesion and motility.

REFERENCE LIST

- (1) Chiorazzi N, Rai KR, Ferrarini M. Chronic lymphocytic leukemia. *N Engl J Med* 2005; 352:804-815.
- (2) Bea S, Lopez-Guillermo A, Ribas M, Puig X, Pinyol M, Carrio A et al. Genetic imbalances in progressed B-cell chronic lymphocytic leukemia and transformed large-cell lymphoma (Richter's syndrome). *Am J Pathol* 2002; 161:957-968.
- (3) Cobo F, Martinez A, Pinyol M, Hernandez L, Gomez M, Bea S et al. Multiple cell cycle regulator alterations in Richter's transformation of chronic lymphocytic leukemia. *Leukemia* 2002; 16:1028-1034.
- (4) Cordone I, Masi S, Mauro FR, Soddu S, Morsilli O, Valentini T et al. p53 expression in B-cell chronic lymphocytic leukemia: a marker of disease progression and poor prognosis. *Blood* 1998; 91:4342-4349.
- (5) Pinyol M, Cobo F, Bea S, Jares P, Nayach I, Fernandez PL et al. p16(INK4a) gene inactivation by deletions, mutations, and hypermethylation is associated with transformed and aggressive variants of non-Hodgkin's lymphomas. *Blood* 1998; 91:2977-2984.
- (6) Cheson BD, Bennett JM, Grever M, Kay N, Keating MJ, O'Brien S et al. National Cancer Institute-sponsored Working Group guidelines for chronic lymphocytic leukemia: revised guidelines for diagnosis and treatment. *Blood* 1996; 87:4990-4997.
- (7) Binet JL, Caligaris-Cappio F, Catovsky D, Cheson B, Davis T, Dighiero G et al. Perspectives on the use of new diagnostic tools in the treatment of chronic lymphocytic leukemia. *Blood* 2006; 107:859-861.
- (8) Crespo M, Bosch F, Villamor N, Bellosillo B, Colomer D, Rozman M et al. ZAP-70 expression as a surrogate for immunoglobulin-variable-region mutations in chronic lymphocytic leukemia. *N Engl J Med* 2003; 348:1764-1775.
- (9) Pinyol M, Hernandez L, Martinez A, Cobo F, Hernandez S, Bea S et al. INK4a/ARF locus alterations in human non-Hodgkin's lymphomas mainly occur in tumors with wild-type p53 gene. *Am J Pathol* 2000; 156:1987-1996.
- (10) Smyth GK. Linear Models and Empirical Bayes methods for assessing differential expression in microarray experiments. *Statistical Applications in Genetics and molecular biology* 2004; 3.

- (11) Krober A, Bloehdorn J, Hafner S, Buhler A, Seiler T, Kienle D et al. Additional Genetic High-Risk Features Such As 11q Deletion, 17p Deletion, and V3-21 Usage Characterize Discordance of ZAP-70 and VH Mutation Status in Chronic Lymphocytic Leukemia. *J Clin Oncol* 2006; 24: 969-976.
- (12) Callet-Bauchu E, Salles G, Gazzo S, Poncet C, Morel D, Pages J et al. Translocations involving the short arm of chromosome 17 in chronic B-lymphoid disorders: frequent occurrence of dicentric rearrangements and possible association with adverse outcome. *Leukemia* 1999; 13:460-468.
- (13) Peterson LC, Lindquist LL, Church S, Kay NE. Frequent clonal abnormalities of chromosome band 13q14 in B-cell chronic lymphocytic leukemia: multiple clones, subclones, and nonclonal alterations in 82 midwestern patients. *Genes Chromosomes Cancer* 1992; 4:273-280.
- (14) Stilgenbauer S, Bullinger L, Lichter P, Dohner H. Genetics of chronic lymphocytic leukemia: genomic aberrations and V(H) gene mutation status in pathogenesis and clinical course. *Leukemia* 2002; 16:993-1007.
- (15) Falt S, Merup M, Gahrton G, Lambert B, Wennborg A. Identification of progression markers in B-CLL by gene expression profiling. *Exp Hematol* 2005; 33:883-893.
- (16) Haran M, Chebatco S, Flaishon L, Lantner F, Harpaz N, Valinsky L et al. Grb7 expression and cellular migration in chronic lymphocytic leukemia: a comparative study of early and advanced stage disease. *Leukemia* 2004; 18:1948-1950.
- (17) Richardson SJ, Matthews C, Catherwood MA, Alexander HD, Carey BS, Farrugia J et al. ZAP-70 expression is associated with enhanced ability to respond to migratory and survival signals in B-cell chronic lymphocytic leukemia (B-CLL). *Blood* 2006; 107:3584-3592.

Table 1: *Clinical and biological characteristics of the CLL patients included in the study.***CLL with clinical progression**

Case	Age(yrs)	Gender	Stage at diagnosis	Stage at progression	Sampling interval (months)	IgV _H	Mutation
CLL1	46	F	A(I)	B(I)	11	VH4-39	Unmutated
CLL2	71	F	A(I)	B(I)	14	VH3-30	Unmutated
CLL3	83	M	A(0)	C(IV)	9	VH3-33	Unmutated
CLL4	54	M	A(I)	B(II)	18	VH1-2	Unmutated
CLL5	71	M	A(I)	C(IV)	6	VH1-69	Unmutated
CLL6	71	F	A(0)	B(I)	9	VH3-7	Unmutated
CLL7	54	F	A(I)	C(IV)	14	VH1-69	Unmutated
CLL8	84	F	A(0)	B(I)	38	VH1-69	Unmutated
CLL9	48	M	A(II)	B(II)	20	VH3-20	Unmutated
CLL10	69	F	A(0)	C(IV)	17	VH3-30	Unmutated
CLL11	59	M	A(II)	B(II)	34	VH3-53	Unmutated
CLL12	86	F	A(0)	C(III)	13	VH1-69	Unmutated
CLL13	55	F	A(I)	B(I)	20	VH4-39	Mutated
CLL14	56	F	A(0)	B(I)	12	VH6-11	Unmutated
CLL15	69	M	A(0)	C(IV)	14	VH3-11	Unmutated
CLL16	51	F	A(I)	B(I)	18	VH1-69	Unmutated

Case	ZAP-70	p53	p16 ^{INK4a}	CGH initial	CGH progressed
CLL1	High	wt	wt	gain 12	gain 12
CLL2	High	wt	wt	not altered	not altered
CLL3	High	wt	wt	not altered	gain (5q21-q23), gain (11pter-p14r)
CLL4	High	wt	wt	del(13q14-q21)	del(13q14-q21)
CLL5	High	wt	wt	del10p	del10p
CLL6	High	wt	wt	not altered	not altered
CLL7	High	wt	wt	not altered	not altered
CLL8	Low	mut	wt	del(9pter-p23), del(17pter-p12)	del(9pter-p23), del(17pter-p12)
CLL9	High	wt	wt	not altered	gain(12)
CLL10	High	wt	del	del (9pter-p23)	del (9pter-p23)
CLL11	Low	wt	wt	gain(12)	gain(12)
CLL12	High	wt	wt	gain(12)	gain(12)
CLL13	Low	wt	wt	del(1q41-qter)	del(1q41-qter)
CLL14	High	wt	wt	not altered	not altered
CLL15	High	wt	wt	not altered	not altered
CLL16	Low	wt	wt	gain(17q22-qter), del (11q14-q24)	gain(17q22-qter), del (11q14-q24)

CLL with stable clinical evolution

Case	Age(yrs)	Gender	Stage at 1 st sample	Stage at 2 nd sample	Sampling interval (months)	IgV _H	Mutation
<i>CLL control 1</i>	n.a	F	A(0)	A(0)	34	VH1-69	Unmutated
<i>CLL control 2</i>	70	F	A(0)	A(0)	40	VH1-69	Unmutated
<i>CLL control 3</i>	59	M	A(0)	A(0)	49	VH2-70	Unmutated

Case	ZAP-70	p53	p16 ^{INK4a}	CGH 1 st sample	CGH 2 st sample
<i>CLL control 1</i>	High	wt	wt	gain(12)	gain(12)
<i>CLL control 2</i>	High	wt	wt	not altered	not altered
<i>CLL control 3</i>	High	wt	wt	gain(4q)	gain(4q)

Figure 1: Summary of the CGH data for the 16 B-CLL cases. Red lines on the left side of the profile indicate loss of the chromosomal material. Green lines on the right side indicate gain of chromosomal material. Alterations acquired by not altered cases at diagnosis CLL3B (violet) and CLL9B (orange) are indicated by an asterisk.

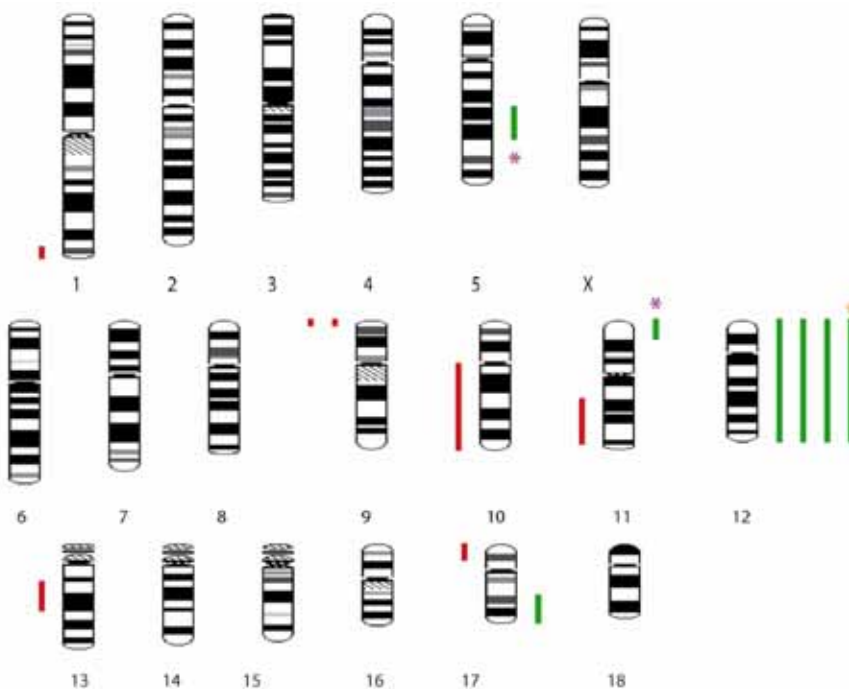
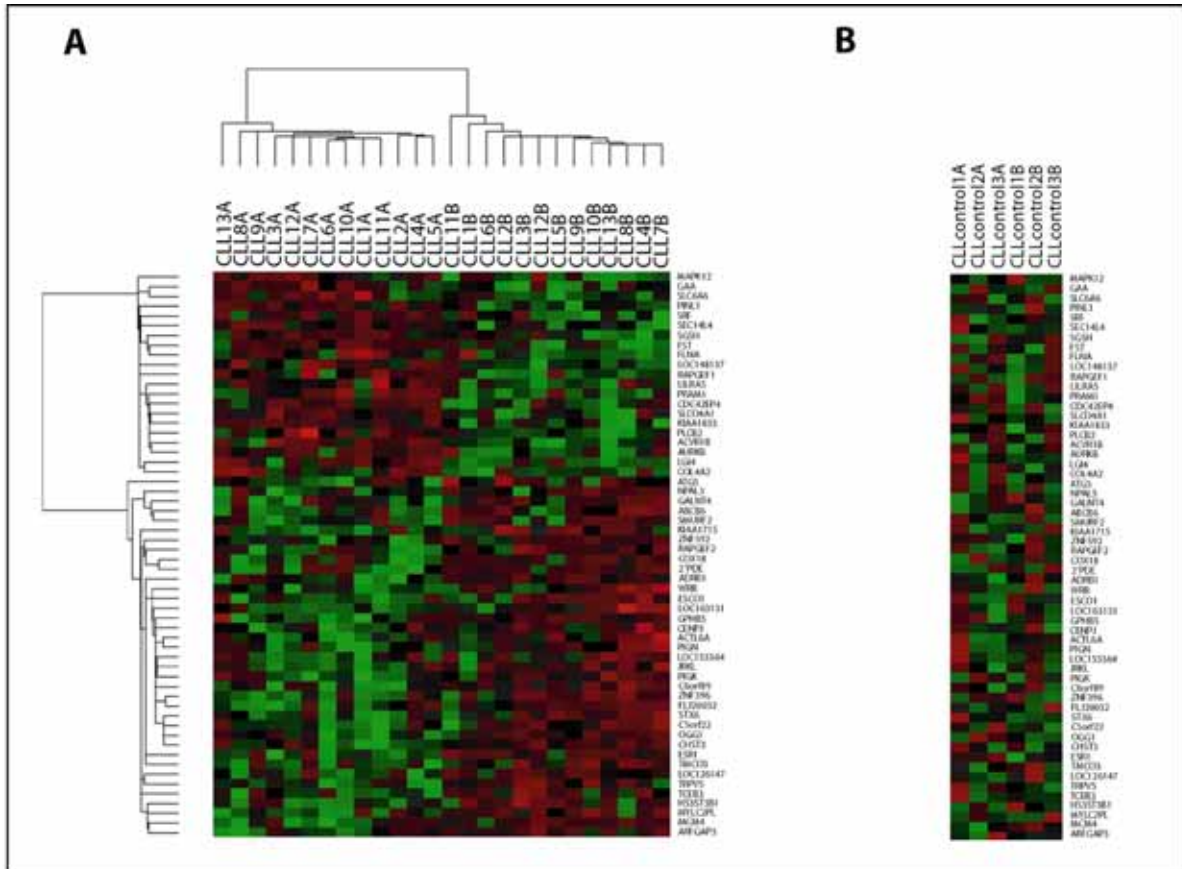


Figure 2: Supervised clustering of the B-CLL sequential samples, performed with the DNA-Chip Analyser (dChip) software and according to the 58 differentially expressed genes found in the microarray data analysis. **A)** CLL with clinical progression; CLLA: initial samples, CLLB: progressed samples. **B)** CLL with stable clinical evolution; CLLA: first samples, CLLB: second samples.



Supplementary table 1: Genes with a significant differential expression between CLL samples at diagnosis and after progression in the supervised analysis of the microarray data.**Overexpressed genes (37)**

Probe set ID	Gene ID	Description	Molecular Function
221659_s_at	MYLC2PL	Myosin light chain 2, precursor lymphocyte-specific	calcium and ion metabolism
1554231_a_at	ZNF396	Zinc finger protein 396	transcription regulation
235091_at	2'-PDE	2'-phosphodiesterase	unknown
229277_at	ADRB1	Adrenergic, beta-1-,receptor	calcium and ion metabolism
203192_at	ABCB6	ATP-binding cassette, sub-family B (MDR/TAP), member 6	mitochondrial activity
1558247_s_at	LOC126147	Hypothetical protein BC018697	unknown
212141_at	MCM4	MCM4 minichromosome maintenance deficient 4	cell cycle and cell growth
220442_at	GALNT4	UDP-N-acetyl-alpha-D-galactosamine	proteoglycan metabolism
1553945_at	GPB5	Glycoprotein hormone beta 5	proteoglycan metabolism
230909_at	COX18	Mitochondrial COX18	mitochondrial activity
32094_at	CHST3	Carbohydrate (chondroitin 6) sulfotransferase 3	proteoglycan metabolism
208267_at	TRPV5	Transient receptor potential cation channel	calcium and ion metabolism
238260_at	RAPGEF2	Rap guanine nucleotide exchange factor (GEF) 2	cell cycle and cell growth
243307_at	ZNF592	Zinc finger protein 592	transcription regulation
205301_s_at	OGG1	8-oxoguanine DNA glycosylase	DNA repair
1570627_at	TCEB3	Transcription elongation factor B (SIII), polypeptide 3	transcription regulation
1566476_at	ARFGAP3	ADP-ribosylation factor GTPase activating protein 3	intracellular protein transport
215551_at	ESR1	Estrogen receptor 1	cell cycle and cell growth
206734_at	JRKL	Jerky homolog-like (mouse)	transcription regulation
235461_at	FLJ20032	Hypothetical protein FLJ20032	unknown
215570_s_at	LOC163131	Hypothetical protein LOC284323	transcription regulation
219048_at	PIGN	Phosphatidylinositol glycan, class N	proteoglycan metabolism
1561908_a_at	HS3ST3B1	Hypothetical protein MGC12916	proteoglycan metabolism
214579_at	NPAL3	NIPA-like domain containing 3	unknown
209707_at	PIGK	Phosphatidylinositol glycan, class K	proteoglycan metabolism
235216_at	ESCO1	Establishment of cohesion 1 homolog 1	cell cycle and cell growth
230298_at	LOC153364	Similar to metallo-beta-lactamase superfamily protein	unknown
225717_at	KIAA1715	KIAA1715	unknown
1552660_a_at	FLJ11193	Hypothetical protein FLJ11193	unknown
220240_s_at	TMCO3	Transmembrane and coiled-coil domains 3	calcium and ion metabolism
202666_s_at	ACTL6A	Actin-like 6A	cell cycle and cell growth
224987_at	C6orf89	Chromosome 6 open reading frame 89	unknown
220885_s_at	CENPJ	Centromere protein J	cell cycle and cell growth
202749_at	WRB	Tryptophan rich basic protein	unknown
214441_at	STX6	Syntaxin 6	protein transport
202512_s_at	ATG5	ATG5 autophagy related 5 homolog	cell cycle and cell growth
227489_at	SMURF2	SMAD specific E3 ubiquitin protein ligase 2	TGF-beta signaling

Probe set ID	Med exp ¹	Fold chg ²	p-value	B
221659_s_at	5.15	1.66	0.041	1.51
1554231_a_at	5.23	1.55	0.022	3.73
235091_at	5.34	1.49	0.033	2.06
229277_at	5.45	1.47	0.029	2.53
203192_at	5.31	1.34	0.036	1.87
1558247_s_at	5.3	1.32	0.044	1.35
212141_at	5.93	1.3	0.049	1.03
220442_at	5.76	1.28	0.049	1.03
1553945_at	5.76	1.24	0.041	1.58
230909_at	5.39	1.2	0.049	1.06
32094_at	6.14	1.2	0.022	3.82
208267_at	5.78	1.12	0.049	1.1
238260_at	6.09	1.09	0.047	1.17
243307_at	5.23	1.08	0.029	2.44
205301_s_at	6.78	0.95	0.024	3.13
1570627_at	5.86	0.93	0.032	2.22
1566476_at	5.22	0.91	0.029	2.36
215551_at	6.39	0.84	0.028	2.78
206734_at	8.11	0.79	0.029	2.56
235461_at	7.19	0.73	0.038	1.78
215570_s_at	7.32	0.65	0.028	2.77
219048_at	7.6	0.6	0.024	3.13
1561908_a_at	6.5	0.57	0.047	1.16
214579_at	7.95	0.56	0.049	1.07
209707_at	9.26	0.53	0.031	2.23
235216_at	7.92	0.51	0.045	1.24
230298_at	8.86	0.49	0.04	1.63
225717_at	7.98	0.48	0.038	1.79
1552660_a_at	8.65	0.48	0.041	1.59
220240_s_at	7.89	0.48	0.044	1.35
202666_s_at	9.25	0.46	0.029	2.41
224987_at	8.22	0.43	0.04	1.64
220885_s_at	7.63	0.42	0.036	1.9
202749_at	9.64	0.41	0.045	1.24
214441_at	8.09	0.4	0.027	2.95
202512_s_at	8.65	0.35	0.042	1.46
227489_at	8.9	0.33	0.047	1.18

¹ Median expression (log2)

² Fold change (log2)

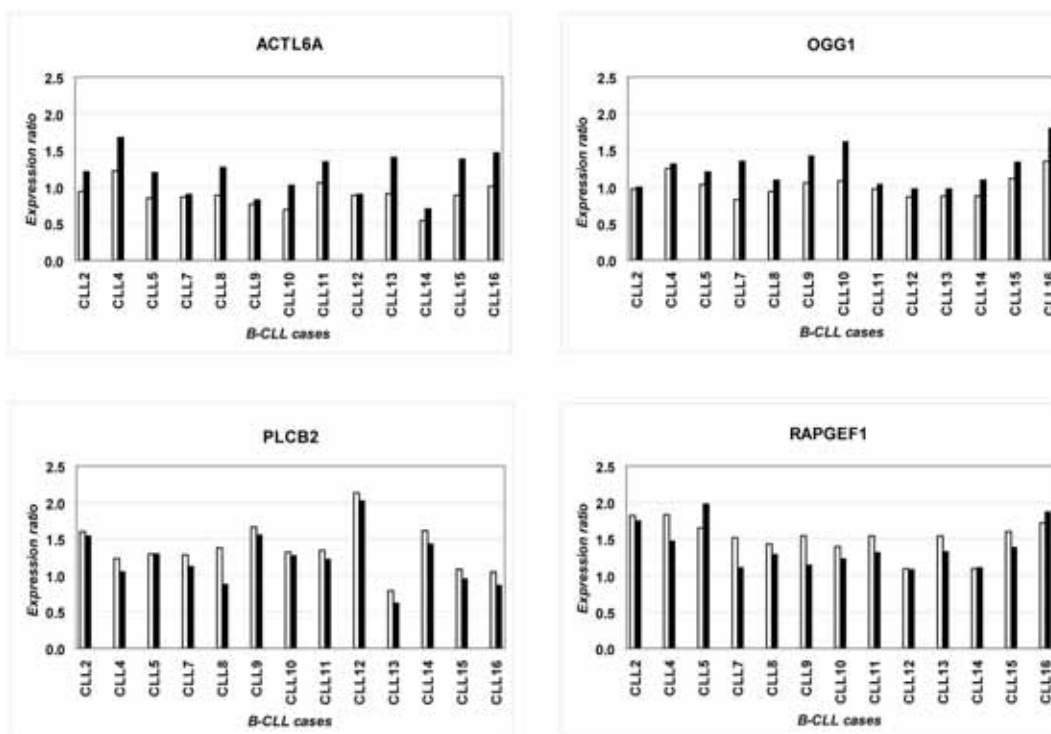
Underexpressed genes (21)

Probe set ID	Gene ID	Description	Molecular Function
232498_at	KIAA1833	Hypothetical protein KIAA1833	unknown
241742_at	PRAM1	PML-RARA regulated adaptor molecule 1	cell adhesion and motility
227821_at	LGI4	Leucine-rich repeat LGI family, member 4	unknown
209464_at	AURKB	Aurora kinase B	cell cycle
208218_s_at	ACVR1B	Activin A receptor, type IB	TGF-beta signaling
206106_at	MAPK12	Mitogen-activated protein kinase 12	MAPK signaling
1554332_a_at	SLCO4A1	Solute carrier organic anion transporter family, member 4A1	transporter activity
204948_s_at	FST	Follistatin	TGF-beta signaling
216402_at	SEC14L4	SEC14-like 4 (<i>S. cerevisiae</i>)	transporter activity
214721_x_at	CDC42EP4	CDC42 effector protein (Rho GTPase binding) 4	cell adhesion and motility
237624_at	COL4A2	Collagen, type IV, alpha 2	cell adhesion and motility
202400_s_at	SRF	Serum response factor	transcription regulation
1555643_s_at	LILRA5	Leukocyte immunoglobulin-like receptor	leukocyte immune response
204293_at	SGSH	N-sulfoglucosamine sulfohydrolase	proteoglycan metabolism
207582_at	PIN1L	Protein NIMA-interacting 1-like	unknown
202812_at	GAA	Glucosidase, alpha	starch and sucrose metabolism
204046_at	PLCB2	Phospholipase C, beta 2	cell adhesion and motility
239474_at	SLC6A6	Solute carrier family 6, member 6	transporter activity
242640_at	LOC148137	Hypothetical protein BC017947	unknown
226389_s_at	RAPGEF1	Rap guanine nucleotide exchange factor (GEF) 1	cell adhesion and motility
214752_x_at	FLNA	Filamin A, alpha (actin binding protein 280)	cell adhesion and motility

Probe set ID	Med exp ¹	Fold chg ²	p-value	B
232498_at	5.94	-1.99	0.024	3.51
241742_at	5.46	-1.76	0.024	3.31
227821_at	5.7	-1.47	0.034	2.01
209464_at	5.19	-1.47	0.044	1.32
208218_s_at	5.54	-1.45	0.024	3.31
206106_at	5.45	-1.36	0.041	1.52
1554332_a_at	5.86	-1.18	0.049	1.04
204948_s_at	6.3	-1.17	0.049	1.07
216402_at	5.93	-1.15	0.029	2.38
214721_x_at	5.48	-1.11	0.043	1.42
237624_at	5.31	-1.11	0.049	1.09
202400_s_at	6.05	-1.07	0.047	1.16
1555643_s_at	6.19	-0.94	0.044	1.33
204293_at	8.27	-0.79	0.045	1.28
207582_at	7.05	-0.71	0.046	1.2
202812_at	8.45	-0.59	0.038	1.78
204046_at	8.77	-0.49	0.029	2.46
239474_at	8.07	-0.46	0.028	2.64
242640_at	7.43	-0.43	0.045	1.23
226389_s_at	10.29	-0.43	0.043	1.42
214752_x_at	10.91	-0.34	0.048	1.13

¹ Median expression (log2)² Fold change (log2)

Supplementary Figure 1: qRT-PCR validation of genes *ACTL6A*, *OGG1*, *PLCB2* and *RAPGEF1*. 10 patients from the microarray study were used for the validation (*CLL2-CLL13*) as well as 3 new patients (*CLL14-CLL16*). White bars correspond to the sample at diagnosis and black bars to the progressed sample. Expression ratios were calculated by the $2^{-\Delta\Delta Ct}$ method using β -glucoronidase (*GUS*) as endogenous control.



Supplementary figure 2: Ingenuity pathway Networks, built for the **A) Overexpressed genes**, and **B) Underexpressed genes** (*Ingenuity Pathways Analysis v.4.0[®]*). The nodes display various shapes, representing different functional classes for the gene product. Straight lines show direct relationships between genes, whereas dotted lines are for indirect relationships. In grey: significant genes included in the given Ingenuity network, *: genes chosen for posterior validation purposes.

